Journal of Hazardous Materials 496 (2025) 139183

Contents lists available at ScienceDirect

Journal of Hazardous Materials

journal homepage: www.elsevier.com/locate/jhazmat

Comparative analysis of asphalt and geomembrane sealing systems for sustainable uranium pile remediation: Insights from hydrological modeling under climate change

Petra Schneider [a,*], Fengqing Li [b], Subin Babu [c]

[a] Magdeburg-Stendal University of Applied Sciences, Breitscheidstr. 2, Magdeburg D-39114, Germany
[b] Magdeburg-Stendal University of Applied Sciences, Breitscheidstr. 2, D-39114 Magdeburg, Germany, and Water Association Burg, Blumenstraße 9B, Burg (bei Magdeburg) D-39288, Germany
[c] Otto Von Guericke University, Magdeburg, Germany

HIGHLIGHTS

- Asphalt and geomembrane seals provide lasting protection for former uranium mining sites.
- Both systems show high impermeability, minimizing radon and water pollution under all climates.
- Asphalt resists desiccation and outperforms geomembranes if vegetation cover fails.
- Hydrologic modeling confirms long-term seepage control, even in worst-case climate scenarios.

GRAPHICAL ABSTRACT

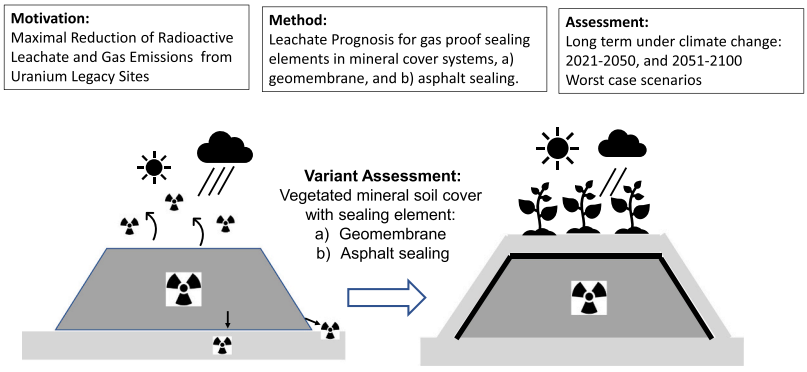

ARTICLE INFO

Keywords:
Uranium legacy sites
Environmentally safe confinement
Long term simulation

ABSTRACT

Uranium ore mining heaps in Saxony and Thuringia (Germany) have been primarily covered with mineral layers as part of remediation efforts. However, aging processes in these covers—driven by climatic factors, vegetation, and root penetration—can create cracks and pathways that increase radon emissions. In residential areas, elevated radon levels may exceed the guideline values set by radiation protection regulations. While asphalt seals and geomembranes are well-established as effective long-term solutions for creating convection-tight surface systems in landfill applications, their use has rarely been considered for uranium legacy sites. This study evaluates the long-term water balance and sealing effectiveness of asphalt and geomembranes at historical uranium mining site under future climate scenarios. Using the Hydrologic Evaluation of Landfill Performance (HELP) model, we simulated water behavior and potential infiltration rates across several sealing configurations, considering current and future climate projections. Our findings reveal that both sealing systems effectively minimize infiltration, surface runoff, and seepage, with negligible infiltration even under worst-case scenarios. The results underscore the robust environmental protection offered by these systems in mitigating radon emission and ensuring long-term environmental safety. This study contributes critical insights for selecting

* Corresponding author.
E-mail addresses: petra.schneider@h2.de (P. Schneider), subin.babu@st.ovgu.de (S. Babu).

https://doi.org/10.1016/j.jhazmat.2025.139183
Received 1 March 2025; Received in revised form 29 May 2025; Accepted 7 July 2025
Available online 11 July 2025

appropriate sealing systems in mining site remediation, offering sustainable solutions that address water conservation, climate resilience, and cleaner production principles.

1. Introduction

The remediation of historical mining sites presents a significant environmental challenge, particularly when addressing the management of waste heap piles. These sites often pose risks to water and air quality, and human health, exacerbated by climate change. As such, selecting effective sealing solutions for these sites is crucial for sustainable land management. This study compares two sealing systems, geomembranes and asphalt, under future climate scenarios to evaluate their ability to prevent infiltration and radon emission. By modeling these systems using the HELP model, we aim to provide evidence-based recommendations for long-term, sustainable remediation strategies that adhere to cleaner production principles. Our research contributes to a growing body of work focused on climate-adaptive remediation technologies that ensure environmental protection and resource efficiency.

Germany was once a major uranium producer, with mining operations beginning in the late 1940s. However, following a decline in demand, production started to decrease in the mid-1970s and eventually ceased after reunification in 1991. Since then, the German federal government has made significant progress in remediating former mining sites, particularly in the regions of Saxony and Thuringia in East Germany. Despite these efforts, some areas still require further remediation, especially in managing tailings facilities and capping heaps [1].

Uranium extraction generates substantial quantities of low-level radioactive residues, typically stored as tailings piles or in nearby industrial tailings facilities [2]. While geotechnical considerations—such as slope stability and compaction—were generally addressed during the construction of these facilities, base sealing was often overlooked. In addition to heavy metals and arsenic, radon emissions are a major environmental challenge associated with waste heap dumps and tailings ponds. Radon is a colorless, odorless, radioactive noble gas that occurs naturally as a decay product of uranium, is chemically inert, and poses significant health risks due to its radioactive emissions. It can be released from dump material through wind and water erosion and can disperse into the atmosphere if the dump material is not adequately sealed. Although atmospheric dilution typically reduces its concentration, elevated radon levels near residential areas can exceed regulatory limits, as defined by radiation protection laws [2]. According to a report by the World Health Organization (WHO), radon exposure is responsible for an estimated 3–14 % of lung cancer cases and is one of the 19 major carcinogens, second only to smoking [3].

Sealing systems that effectively control convective air and gas flows, while preventing the migration of hazardous substances, are crucial for mitigating environmental impacts. Their main application field is landfill closure and rehabilitation. Recent research on gas emissions from waste sites has primarily focused on landfill gas (LFG) emissions and the role of capping systems in minimizing environmental harm, an issue long addressed in geotechnical engineering. Przydatek et al. (2024) highlighted that environmental factors such as precipitation, relative humidity, and air temperature significantly influence landfill gas emissions during both the operational and post-operational phases of municipal waste landfills. These factors directly impact the generation of landfill gases, underscoring the importance of maintaining proper cover systems to minimize emissions [4]. Conventional capping systems for landfills comprise mineral capping systems, geosynthetic clay liners and asphalt seals. Their main function is to prevent gas emissions from the landfill body to the surface, and precipitation input from the surface to the landfill body. The available literature on other sealing systems than mineral capping systems and geosynthetic clay liners to minimize gas emissions from uranium legacy sites is very limited. Hartley et al. (1980) investigated the use of asphalt emulsion to contain radon and radium in uranium tailings and found that a radon flux reduction of greater than 99 % can be obtained using either a poured-on/sprayed-on seal (3.0–7.0 mm thick) or an admix seal (2.5–15.2 cm thick) [5]

In this study, we assess convection-tight sealing solutions for uranium mining heaps using hydrological modeling that integrates physical principles of fluid flow, material properties, and environmental factors. However, to date, few studies have focused specifically on convection-tight sealing systems for uranium mining heaps. This gap in the literature may be due to the relatively low levels of radon exhalation from heaps that are located far from residential areas, and compared to exhalation levels of tailings ponds. In contrast, in the case of the uranium heaps in the Ore Mountains of Eastern Germany, where human settlements are located in close proximity, the risk to inhabitants is more pressing. Therefore, one motivation of the study was to assess the feasibility of transferring landfill sealing solutions to uranium heaps, particularly for asphalt sealings. Ozbay et al. (2021) emphasize that poorly managed landfills pose a heightened health risk to nearby communities [6], which applies also for uranium heaps. Therefore, this study employs water balance modeling of convection-tight sealing systems as a proxy to estimate the risk of (a) leachate formation and (b) potential radon exhalation flow paths through the sealing layer.

Several studies have investigated the migration behavior of gases through different sealing materials, including compacted clay and synthetic liners. For instance, Scheutz et al. (2004) demonstrated the attenuation of methane and volatile organic compounds (VOCs) in landfill covers, which share similar challenges with uranium heap management in terms of permeability control and gas leakage [7]. Similarly, Wang et al. [8] used numerical analysis to optimize ventilation in underground environments, focusing on the dispersion of radon, which has similar properties to gases found in uranium mining operations. Their findings emphasized the importance of sealing integrity and ventilation control in limiting the spread of hazardous gases [8]. Radon flow can be effectively reduced through convection-tight sealing systems however such systems are very rarely applied in uranium mining remediation yet.

The performance of various sealing materials has also been studied in different contexts. Manheim et al. reviewed global emissions from municipal solid waste landfills and identified the critical role of capping systems in controlling gas emissions. They noted that the choice of sealing materials significantly affects the long-term effectiveness of containment strategies [9]. Albright et al. (2006) assessed the field performance of compacted clay landfill covers, providing insights into the longevity and efficiency of natural sealing materials in controlling gas flow and moisture seepage [10]. Additionally, Manheim et al. (2021) found that gas emissions from sealing covers were inversely correlated with the void ratio of the cover material, highlighting the importance of minimizing voids to reduce radon release [11]. In a similar study, Lydia et al. [12] concluded that site-specific cover systems are the most effective in post-mining landscapes, suggesting that tailored approaches to sealing are more successful than using standardized liners [12]. In the context of uranium legacy remediation in Eastern Germany, usually mineral capping

The impact of climate change on sealing systems has become an increasing area of concern. Hotton et al. [13] examined the role of capillary barrier systems in controlling acid generation in mining waste piles, noting how shifts in precipitation and temperature patterns could compromise the effectiveness of covers [13]. This issue is particularly relevant for uranium mining heaps, where the long-term stability of covers is essential for minimizing environmental contamination.

Permeability of sealing materials is another key factor in designing

effective covers. Beck-Broichsitter et al. [14] found that artificial soil compaction affects the anisotropy of air permeability in landfill capping systems, with the uniformity of compaction playing a vital role in the performance of sealing layers [14]. Hanson et al. [15] observed that emissions decreased as soil cover transitioned from coarser to finer materials, a finding that is especially relevant for uranium mining heaps, where permeability control is critical for minimizing gas and liquid migration [15].

Emerging studies on alternative sealing materials, such as those based on industrial by-products, show promise for enhancing the sustainability of landfill and heap cover systems. Ling et al. (2024) demonstrated that using sewage and incineration by-products in landfill covers can improve sealing efficiency and reduce environmental impacts [16]. Similarly, Al-Soudany et al. [17] showed that incorporating recycled industrial waste into sealing materials can reduce reliance on natural resources like clay, offering a more sustainable approach [17]. These materials could provide cost-effective solutions for uranium mining heaps, where sustainable remediation is increasingly sought. Daramola et al. [18] found that blending lateritic soils with bentonite, fly ash, sawdust, and mine tailings enhanced their geotechnical properties, making them more suitable as liner materials [18].

The present research highlights the importance of efficient sealing systems in managing gas emissions and seepage from mining heaps. Building on these findings, this study applies hydrological modeling to evaluate the performance of different convection-tight sealing solutions. The goal is to identify optimal strategies for controlling gas migration and preventing environmental contamination at uranium mining sites. By comparing various sealing materials under simulated environmental conditions, this research aims to provide actionable insights into the development of more effective heap cover systems.

In addition to physical sealing systems, alternative remediation approaches such as phytoremediation have shown promise in stabilizing radioactive contaminants through plant uptake and root-zone immobilization. For instance, Stojanovic et al. [19] demonstrated the potential of certain hyperaccumulator species to reduce uranium mobility in contaminated soils [19]. However, such biological methods often require longer timeframes and favorable site-specific conditions, which limits their applicability in high-risk zones. Likewise, passive treatment systems, including constructed wetlands and reactive barriers, have been explored for their ability to attenuate contaminants in mine drainage, offering energy-efficient and low-maintenance alternatives [19–22]. In recent years, the use of industrial by-products such as fly ash, blast furnace slag, and incinerator residues has gained attention as sustainable sealing components. Studies have shown that these materials can enhance barrier performance while reducing reliance on natural clay resources [16,17]. Nevertheless, their long-term performance under extreme climatic conditions is still being evaluated. Against this background, convection-tight sealing systems such as asphalt and geomembranes remain practical and robust solutions for managing radon emissions and seepage in uranium legacy waste heaps.

In Saxony, remediation efforts for waste dumps have focused on developing surface sealing systems to minimize gas exchange between the tailings and dump material and ambient air, while also reducing seepage, in compliance with state-of-the-art standards and mining law requirements. These systems include single-layer, dual-layer, and multilayer mineral covers, as well as partial covers [23]. Berger et al. (2019) demonstrated that liner performance improves with increased thickness and the use of low hydraulic conductivity materials [24]. Convection-tight surface seals aim to obstruct radon transport from waste heap dumps into the atmosphere, addressing observed reductions in sealing performance over time, particularly in mineral waterproofing systems (5–15 years post-construction) [2]. Asphalt seals (AS) and geomembranes (GM) are recognized as effective sealing elements. The remediation goal is to sustainably reduce radon emissions from tailings piles or waste heap dumps, ensuring that the effective reference dose remains below the 1 mSv/a limit [25].

To evaluate the dynamics, load-bearing capacity, and effectiveness of various remediation strategies, a numerical investigation was conducted using a synthetic model of the waste heap dump. The Hydrologic Evaluation of Landfill Performance (HELP 3.95D) model was employed to simulate the performance of different sealing systems. The HELP model, a widely used tool for assessing water balances in landfill cover and liner systems, was applied to simulate the leachate formation and compare the performance of AS and GM with a previously used mineral sealing layer [26]. The model incorporated diverse weather data parameters to simulate leachate rates through soil layers and track changes in the leachate head over time. The HELP model has gained widespread recognition over the past decade as a robust and versatile tool for evaluating water balance in landfill systems [27]. For example, Alslaibi et al. (2013) used the HELP model in combination with the Water Balance Model (WBM) to assess leachate generation and percolation at the Deir Al Balah landfill, finding that the results from both models were closely aligned [28]. This highlights the model's reliability and relevance for simulating hydrological processes in various landfill settings

2. Materials and methods

2.1. General approach

The methodology for this study centers on numerical simulation using the HELP 3.95D model to evaluate the long-term water balance and sealing performance of two alternative cover systems, geomembrane (GM) and asphalt seal (AS), at uranium mine tailings sites. The model allows estimation of key hydrological variables such as infiltration, surface runoff, leachate generation, and evapotranspiration under layered soil systems. The analysis focused on a synthetic tailings pile located in Saxony, Germany, with a layered structure representative of field remediation practices. Climatic inputs for the model were derived from historical data (1999–2020) and future climate projections (2021–2100) under three RCP scenarios. A total of eleven configurations were tested, including uncovered, current state, and convection-tight sealing designs with and without worst-case defects. The overall aim was to assess the long-term hydraulic effectiveness of the sealing systems under varying climate conditions and identify the most robust option for radon and leachate control.

The primary objective of this study was to compare different design alternatives for sealing systems based on site-specific water balance data, influenced by local climate conditions. The HELP 3.95D model was used to simulate multiple hydrological processes with a daily time step. The HELP 3.95D model employs a series of computational routines to simulate the hydrological behavior of landfill cover systems. These routines are designed to model various water movement processes within the landfill profile, accounting for factors such as precipitation, evapotranspiration, runoff, infiltration, and drainage. The key computational routines in HELP 3.95D are:

Evapotranspiration Calculation: HELP 3.95D computes both potential and actual evapotranspiration based on meteorological data and vegetation parameters. The model considers the leaf area index (LAI) and the growing season to estimate water loss through plant transpiration and soil evaporation.

Runoff Estimation: The model calculates runoff by evaluating the precipitation intensity, soil infiltration capacity, and surface characteristics. It uses empirical equations to estimate the portion of rainfall that becomes surface runoff, which is crucial for designing drainage systems.

Infiltration and Percolation Modeling: HELP 3.95D simulates vertical water movement through the landfill cover layers. It accounts for infiltration rates influenced by soil properties and layer compositions, and models percolation through barrier layers, considering factors like hydraulic conductivity and layer thickness.

Lateral Drainage and Leachate Collection: The model includes routines to estimate lateral drainage of leachate via drainage layers. It calculates the efficiency of leachate collection systems by considering

the permeability of materials and the configuration of drainage layers. With HELP, 1–20 layers can be modeled in a landfill profile. There are four layer types:

- Vertical percolation layers (VPL): Flow in percolation layers is modeled as vertical, downward, unsaturated, or saturated flow driven solely by gravity or a dam.
- Lateral drainage layers (LDL): These are layers directly above barriers that allow lateral drainage into a drainage system.
- Barrier soil layers (BSL): These are designed to limit vertical infiltration (seepage, percolation, or leakage).
- Plastic sealing membranes (geomembranes, GML): are practically impermeable synthetic membranes that reduce the area through which water can seep to a very small proportion of the total area in the vicinity of manufacturing and installation defects (punctures, cracks, faulty seams).

Leakage through Liners: HELP 3.95D assesses the potential for water leakage through geomembrane and barrier soil liners. It incorporates factors such as liner defects, construction quality, and material properties to estimate leakage rates, which are critical for evaluating the containment effectiveness of landfill designs.

Soil Moisture and Layer Interactions: The model simulates the interactions between different soil layers, including moisture storage and movement. It considers the effects of layer composition, compaction, and permeability on the overall water balance within the landfill system.

These routines collectively enable HELP 3.95D users to perform detailed water balance simulations, supporting the design and evaluation of landfill cover systems to prevent groundwater contamination and ensure environmental compliance.

2.2. Fluid transport in mine dumps

2.2.1. Radon

Radon (Rn-222) is formed by the radioactive decay of radium (Ra-226) in the uranium-radium decay series. The volume-related release of radon into the pore volume of the waste dump material Liu et al. [29] is

$$P = ER\lambda\rho_b$$

P Radon production rate in Bq/(m³s)
λ Decay constant of Rn-222 (2.1E-6 s-1)
E Emanation coefficient of the waste pile material
ρb Bulk density of the waste pile material
R Specific activity of Ra-226 in the waste pile material

Radon in the pore air of the waste pile material is available for convective and diffusive transport to the waste pile surface. Radon removal is essentially linked to convective air flow, which is driven by a thermal gradient between the pore air in the waste pile material and the ambient air.

To calculate the pressure difference along a streamline, the simplifying assumption of a uniform temperature inside the heap and in the outside air, as well as a steady state, is usually used. The pressure difference Δp between the inside and outside of the heap at the heap base [30] is described by

$$p = \rho H\alpha g\Delta T$$

ρ Air density at mean atmospheric pressure (1013 hPa)
g Gravitational acceleration
α Coefficient of air expansion (0.0037 /K) at a temperature of 283.15 K
ΔT Temperature difference between the interior of the dump and the outside air
H Geodetic height difference between the dump base and the plateau in m.

The flow velocity (filter velocity) νB along a streamline in the dump material can be determined using [31]:

$$\nu_B = k_H(\Theta) \quad \frac{\Delta p}{\eta L}$$

νB Flow velocity along a streamline
η Viscosity of air (1.8E-5 Pa s)
$k_H(\Theta)$ Saturation-dependent permeability of the dump material; for simplification, dry dumps can be assumed for surface-sealed mine dumps

$$J_k = \frac{P \quad \nu_B}{\lambda} \quad \left(1 - \exp\left[\frac{-\lambda\varepsilon L}{\nu_B}\right]\right)$$

Δp Pressure difference along the streamline
L Length of the "streamline" inside the mine dump

The radon flux density escaping from the dump base or the dump plateau, depending on the sign of the temperature difference, is then, assuming dry tailings material:

However, for further considerations regarding the effectiveness of surface sealing, a comparison between uncovered and covered dumps was planned, so the exact proportions of convective flow across the entire dump surface are irrelevant. The discharge of radon from uranium mining dumps leads to increased activity concentrations of radon and radon decay products, particularly at the dump base, which in turn can lead to increased exposure of members of the public. The discharge of cold air at the dump base, which is colder than ambient temperature and has a high radon activity concentration, and thus increased exposure of the population living there, is primarily limited to the summer months. In the winter months, the flow conditions are reversed, and the air inside the dump, which is warmer than ambient temperature, rises and escapes onto the dump plateau. With regard to the exposure of the general public, convective radon discharge at the dump base is therefore particularly relevant during the summer months.

Under the assumptions typical for uranium mining dumps in the Ore Mountains: permeability of the dump material 1E-9 m², temperature difference between the dump interior and ambient air 10 K, geodetic height difference: 50 m, specific activity of Ra-226 1 Bq/g, density of the dump material: 2000 kg/m³ , porosity of the dump material 0.31, emanation coefficient of the (dry) dump material 0.1, the radon flux density coupled to a convective air flow is in the order of 10 Bq/(m²· s) [29].

Convective radon evaporation can only be reduced by sealing with a permeability of no more than 1E-12 m². The diffusive component of radon evaporation from mine dumps is generally at least an order of magnitude lower than convection. With the parameters specified above and a diffusion constant of the dump material of 3E-6 m²/s, the current density of the diffusive radon evaporation is approximately 5E-1 Bq/(m²·s), Zakaria et al. [32]. The diffusive component was therefore not considered further. Effective measures to reduce the radon activity concentration at the dump toe are therefore linked to the prevention or reduction of convection currents within the dump material. The generally two feasible convection-tight technical sealing variants are geomembranes (GM) and asphalt sealings (AS), as these types of sealings are used in landfill capping

2.2.2. Water transport as a proxy for convection-tight sealing systems

The general water balance of a heap is characterized by the following components:

P = AE + Qs + Ql + Dl + Ds + (R - C)
P→Precipitation
AE→actual Evapotranspiration
Qs→Runoff from the surface
Ql→lateral runoff from the recultivation layer
Dl→lateral drainage from the drainage layer
Ds→drainage from the sealing layer
R - C→Change in water content in the sealing system = retention - consumption

Precipitation is the most reliably determinable quantity. The result of the water balance calculation is the runoff quantity from the sealing layer, i.e. the amount of water that penetrates into the waste body after its sealing. Each layer has its own water balance.

The basic equation for saturated flow in soil layers is Darcy's law:

$$Q = k\ A\frac{\Delta h}{l}$$

$$q = \frac{Q}{A} = K * I$$

$$k = \frac{Q/A}{\Delta h/l}$$

with Q- Flow rate
q - Flow velocity
A – Area of soil perpendicular to the flow
Δh – Hydraulic head difference
l – flow length
i – Hydraulic gradient
K – Permeability coefficient, hydraulic conductivity

The hydraulic conductivity K is a combined material property of porous medium and liquid, which can be described as follows [30]:

$$K = k * \frac{g\rho}{\eta} = k * \frac{g}{\upsilon}$$

with k – Specific permeability coefficient, specific hydraulic conductivity
g – Acceleration due to gravity
η – Dynamic viscosity of the fluid
υ – Kinematic viscosity of the fluid

The hydraulic conductivity K is a combined material property of porous medium and liquid, which can be described as follows [30]:

$$K = k * \frac{g\rho}{\eta} = k * \frac{g}{\upsilon}$$

with k – Specific permeability coefficient, specific hydraulic conductivity
g – Acceleration due to gravity
η – Dynamic viscosity of the fluid
υ – Kinematic viscosity of the fluid

In purely mineral cover layers, similar physical processes occur as in the unsaturated soil zone. The forces that cause the directed movement of water are:

- The vertically downward gravitational force (gravitational potential)
- The upward capillary suction tension (matrix potential).

When precipitation water hits a capping system, the upper soil zones are initially saturated. Further water inflow causes the moisture front to advance to greater depths. The hydraulic conductivities at the respective saturation level of the soil zone are crucial for water transport. If the seepage water encounters an area with lower hydraulic conductivity, such as a sealing element, the seepage movement slows down, and stagnant water can form. If the precipitation exceeds the amount that can infiltrate the soil, the water flows away above ground. Capillary rise, a water transport against gravity caused by differences in soil suction tension, is important for water movement in surface sealing systems. This effect is amplified by water removal by plant roots (transpiration).

In order to calculate water movement or the temporal development of water saturation at different depths in the capping system, the hydraulic properties of the materials must be identified. The hydraulic properties of unsaturated soils primarily refer to the relationship between soil moisture tension and water content, as well as the dependence of hydraulic conductivity on water content or soil moisture tension (pF). The pF value is defined as the decimal logarithm of the positive value of soil moisture tension in cm. The actual hydraulic conductivity of a sealing system in the medium term depends on the fine soil content (silt and clay fraction) and the resulting field capacity. Whether plants can develop suction tension forces in the pore space depends on the pore size and the bulk density. As determined by Heinze et al. [33], root penetration in cover layers ends at soil capping layers with a bulk density of > 1.8 g/cm^3.

The recultivation layer therefore represents an essential component in the surface protection and recultivation of landfills and dumps. Parameters such as thickness, soil type, vegetation, installation conditions, usable field capacity, permanent wilting point, air capacity as well as installation technology and installation density play a decisive role in the long-term functionality. Two main purposes of using vegetation parameters are 1) estimating potential and actual evaporation; and 2) determining the runoff curve number.

Evapotranspiration (ET) is the process of water loss through evaporation from the soil profile and other surfaces, as well as through transpiration from plants. Pure evaporation occurs from open water surfaces or from soil surfaces and vegetation, whereas the process of transpiration is the removal of water from the soil by plant roots, which then evaporates into the atmosphere through the plant leaves. Potential evapotranspiration (PE) is the maximum amount of evaporation that occurs during a day due to the unlimited removal of water from the soil by the atmosphere. In the HELP model, potential evapotranspiration is calculated based on a modified Penman equation using the following equations.

$$PET_i = \frac{LE_{si}}{L_V}$$

and

$$L_V = 59.7 - 0.0564 \quad T_{Ci}$$

where *PETi* is the potential evapotranspiration on day i (mm); *LEsi* is the available energy for potential evapotranspiration on day i (MJ/mm2); LV is the latent heat of evaporation (MJ/mm2/mm); and *TCi* is the mean air temperature (°C).

Actual evapotranspiration (*AE*) is the amount of evapotranspiration that occurs when there is a limit to the amount of available water. The actual evapotranspiration (*AETi*) for segment j on day i is the sum of actual soil water evaporation (*ESWi*) and actual plant transpiration (*EPi*) from segment j.

$$AET_i\ (j) = ESW_i\ (j) + EP_i\ (j)$$

The actual total evapotranspiration (*TEi*) on day i results from the summation of the subsurface evapotranspiration (*ESSi*) and the surface evaporation (*ESi*).

$$TE_i = ES_i + ESS_i$$

In the HELP model, potential and actual evapotranspiration were calculated based on the following required information:

- In the study area, the depth of the evapotranspiration zone is 100 cm (recultivation type 1, namely grass cover + 20 cm topsoil + 80 cm subsoil) and 250 cm (recultivation type 2, namely tree cover + 30 cm topsoil + 270 cm subsoil), respectively.
- The maximum leaf area index value (area/area) is 5 for recultivation type 1 and 7 for recultivation type 2.
- The starting date of the growing season in Aue is April 16, and the ending date of the growing season is October 18.

The relationship between runoff and precipitation is calculated in the HELP model based on the SCS (Soil Conservation Service) curve number method according to the following:

$$Q = \frac{P - 0.2 \quad S^2}{P + 0.8 \quad S}$$

where Q is the actual runoff or excess precipitation (mm), P is the actual precipitation depth (mm), and S is the maximum potential retention after the onset of runoff (retention parameter) (mm).

2.3. Required model input data

The model requires daily input data for precipitation, air temperature, and solar radiation, spanning from 1 to 100 full calendar years. Additional parameters for calculating evaporation and factors such as soil and material properties, as well as the layer structure and location, were also incorporated into the model. A schematic overview of the data processing and modeling framework, along with the initial data set, is provided in Fig. 1.

2.4. Modeling scenarios and settings

2.4.1. Modeling scenarios

In this study, 11 distinct scenarios were considered to evaluate the water balance and effectiveness of different sealing strategies for uranium mining heaps. The scenarios include baseline conditions, current sealing configurations, and alternative designs with varying sealing elements. These scenarios are as follows:

Reference Model: A baseline scenario with no cover or sealing on the uranium waste heap dump.

Current State 1: A single-layer cover, representing the existing configuration of uranium waste heap dumps in Aue, Germany.

Current State 2: A two-layer cover, representing the existing configuration of the uranium waste heap dump in Königstein, Germany.

A1–A4: Scenarios using geomembranes (GM) as the convection-tight element, approved by the BAM (German Federal Material Proofing Agency).

B1–B4: Scenarios using asphalt sealing (AS) as the convection-tight element, assessed for suitability by the LAGA (German Waste Association).

For both A (geomembranes) and B (asphalt sealing) variants, variations in the layer structure were included to reflect standard practices. These modifications primarily involved using plastic drainage elements (PDE) as a substitute for primary raw material drainage layers, or adjusting the thickness of the recultivation layer. All configurations represent common practical designs for conventional landfill covers, and have not yet been applied to uranium waste heap dumps.

In the HELP model, the curve number values were 71.15 for the current state and recultivation type 1 cases, as well as 59.27 for the recultivation type 2 cases, respectively. The curve number was estimated based on the soil database using the soil type (moderately compacted sandy loam), the vegetation type (moderate grass cover for recultivation type 1 and excellent grass cover for recultivation type 2), a slope gradient of 24.2 %, and a slope length of 101.9 m. In the zero model, the curve number value was determined to be 20.

Layer Structures for Sealing Scenarios

The following layer structures for the sealing scenarios were considered, based on project findings to date:

A) ***Convection-tight Element: Geomembrane (GM) (certified by the Federal Material Proofing Agency)***

- A1 - GM (2.5 mm) - PDE (~8 mm) - Recultivation soil (min. 0.8 m subsoil + 0.2 m topsoil)
- A2 - GM (2.5 mm) - PDE (~8 mm) - Recultivation soil (min. 2.7 m subsoil + 0.3 m topsoil)
- A3 - GM (2.5 mm) - Protective geotextile (1200 g/m^2, approx. 8 mm) - Mineral drainage (16/32 mm) - Geotextile (300 g/m^2, approx. 3 mm) - Recultivation soil (min. 0.8 m subsoil + 0.2 m topsoil)
- A4 - GM (2.5 mm) - Protective geotextile (1200 g/m^2, approx. 8 mm) - Mineral drainage (16/32 mm) - Separating geotextile (300 g/m^2, approx. 3 mm) - Recultivation soil (min. 2.7 m subsoil + 0.3 m topsoil)

B) ***Convection-tight Element: Asphalt Sealing (AS) (certified by the Federal Material Proofing Agency)***

- B1 - Landfill asphalt base layer - AS 16 T-DA (min. 6 cm) - Landfill asphalt sealing layer - AC 11 D-DA (min. 4 cm) - PDE (~8 mm) - Recultivation soil (min. 0.8 m subsoil + 0.2 m topsoil)
- B2 - Landfill asphalt base layer - AS 16 T-DA (min. 6 cm) - Landfill asphalt sealing layer - AC 11 D-DA (min. 4 cm) - PDE (~8 mm) - Recultivation soil (min. 2.7 m subsoil + 0.3 m topsoil)
- B3 - Landfill asphalt base layer - AS 16 T-DA (min. 6 cm) - Landfill asphalt sealing layer - AC 11 D-DA (min. 4 cm) - Mineral drainage (16/32 mm) - Separating geotextile (300 g/m^2, approx. 3 mm) - Recultivation soil (min. 0.8 m subsoil + 0.2 m topsoil)
- B4 - Landfill asphalt base layer - AS 16 T-DA (min. 6 cm) - Landfill asphalt sealing layer - AC 11 D-DA (min. 4 cm) - Mineral drainage

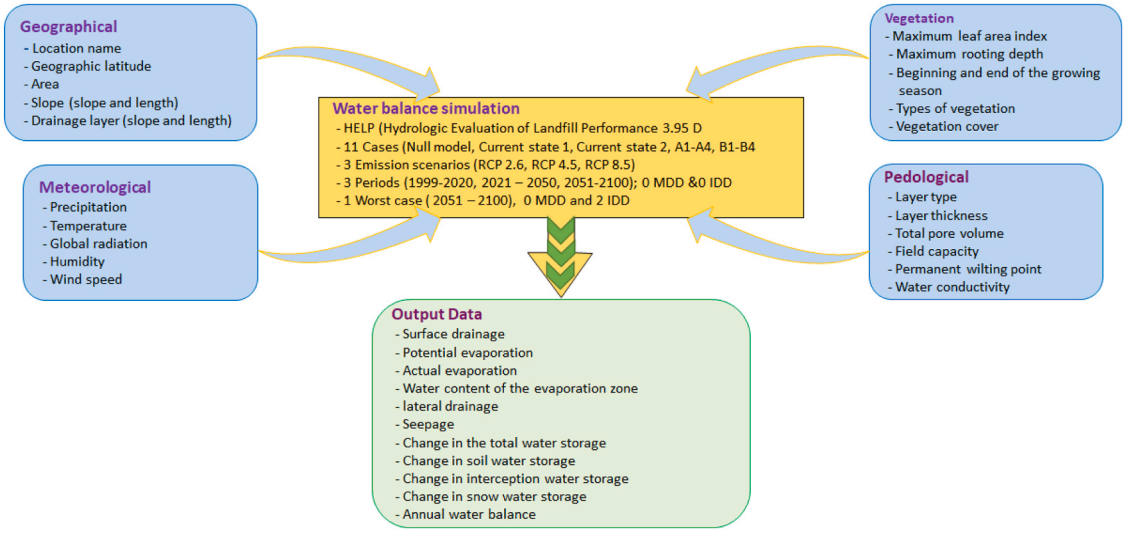

Fig. 1. Scheme for data processing, modeling, and list of source data. RCP = representative concentration path; MDD = Manufacturing defect density; IDD = installation defect density.

(16/32 mm) - Separating geotextile (300 g/m^2, approx. 3 mm) - Recultivation soil (min. 2.7 m subsoil + 0.3 m topsoil)

2.4.2. Timeframes and defect considerations

The study period was divided into three timeframes to assess the long-term performance of the sealing systems:

1999–2020: Observed climate data (Provided by the German Weather Service, DWD).

2021–2050: Climate forecast data (Obtained from the Regional Climate Information System (ReKIS), using the CMIP5_CanESM2_EPISODES-2018 prediction model).

2051–2100: Long-term forecast data (Obtained from the Regional Climate Information System (ReKIS), using the CMIP5_CanESM2_EPISODES-2018 prediction model), including worst-case scenarios.

Given that the HELP model does not account for aging effects of waterproofing elements, a worst-case scenario for 2051–2100 was considered, incorporating potential manufacturing defects and installation defects. These defects are defined as follows:

- Manufacturing Defect Density (MDD): For Germany, MDD is effectively eliminated through strict quality assurance in landfill construction and was set to 0 for all scenarios.
- Installation Defect Density (IDD): Localized damage to geomembranes over long periods is possible, so an IDD of 2 defects (holes of 0.5 mm) per GM hectare was used for the period 2051–2100. This defect density assumes perforations with a maximum diameter of 1 mm, allowing both fluids and radon to permeate.

2.4.3. Climate scenarios

The modeling scenarios utilized three different Representative Concentration Pathways (RCP) for the climate forecast:

- RCP 2.6: Represents maximum climate protection efforts, with global emissions peaking between 2010 and 2020, followed by a substantial decline.
- RCP 4.5: Emissions peak around 2040 and gradually decline thereafter.
- RCP 8.5: Represents a "business as usual" scenario, with emissions continuing to rise throughout the 21st century.

Water balance simulations were conducted for the years 1999–2100, based on two data sources:

- Observed Climate Data (1999–2020): Provided by the German Weather Service (DWD).
- Predicted Climate Data (2021–2100): Obtained from the Regional Climate Information System (ReKIS), using the CMIP5_CanESM2_EPISODES-2018 prediction model.

The climate scenarios were applied across the different timeframes and emission scenarios (RCP 2.6, RCP 4.5, and RCP 8.5), with a specific focus on the worst-case scenario for the period 2051–2100.

The wind speed depends largely on the height above ground and the ambient conditions. The standard measurement height for wind speed at the DWD and ReKIS is 10 m above ground. HELP requires the wind speed at a height of 2 m above ground. The following equation was used to calculate the wind speed at a height of 2 m:

$$v_2 = v_x \times \frac{4,2}{\ln(x) + 3,5}$$

where v2 is the wind speed at 2 m height and x is 10.

2.4.4. Site-specific data

The model was applied to Aue / Bad Schlema uranium waste heap dumps in Saxony, Germany, as a model case. Geographical and vegetation characteristics specific to this site were incorporated into the simulations, along with historical and forecast meteorological data from the Saxon State Office for the Environment, Agriculture, and Geology (LfULG). This ensured that the model accurately reflected site conditions and local climate patterns.

2.4.5. Soil Characteristics input data

The German version of the Hydrologic Evaluation of Landfill Performance (HELP) model, referred to as HELP 3.95D, is an adaptation of the original U.S. Geological Survey model (HELP 3.07), modified to account for site-specific climatic and soil conditions in Germany. While the U.S. version incorporates 44 predefined soil material types classified according to the USDA Soil Texture Classification and the Unified Soil Classification System (USCS), the German adaptation underwent comprehensive validation efforts to ensure its applicability to typical German soils and landfill designs. The original U.S. HELP model classifies soil types as follows:

- Low-density soils: Types 1–15 and 21
- Moderate-density soils: Types 22–29
- High-density soils: Types 16 and 17
- Geomembranes and geotextiles: Types 35–42
- Waste materials: Types 18–19, 30–33

To ensure the validity and reliability of HELP 3.95D under German conditions, the model was calibrated and tested using German soil physical properties, including local permeability coefficients, porosity, field capacity, and bulk density values derived from extensive datasets [34]. The validation process involved Berger et al. [35,36].

- Comparison of model outputs with measured field data from German landfills.
- Sensitivity analyses under typical German precipitation, evaporation, and temperature regimes.
- Integration of locally relevant material parameters, particularly for compacted mineral liners and geosynthetic elements used in German landfill engineering.

The validation demonstrated that HELP 3.95D can accurately simulate vertical water movement and leachate generation in German climatic and pedological settings, making it a reliable tool for hydrological landfill performance assessments in Germany.

Water moves downward through the vertical unsaturated soil layers driven by gravity. In the HELP model, the unsaturated hydraulic conductivity of waste and soil layers is calculated following Campbell's method (1974), which is based on Darcy's law. The values for layer type, layer thickness, total pore volume, field capacity, permanent wilting point, and saturated hydraulic conductivity (kf value) are required for VPL, LDL, and BSL. However, only the values for layer type, layer thickness, and saturated hydraulic conductivity are required for GML. For drainage layers, the following two additional design parameters are required:

- The maximum horizontal drain spacing: the length of the projection of the flow path from the highest slope point to the drain on the horizontal. The design length in this study is 100 m.
- The displacement head: the slope of the drainage layer base or the surface of the liner underlying the drainage layer, which corresponds to the slope of the flow path. The design slope in this study is 5 %.

The program also requires values for the density of fabrication defects (FD) and installation defects (ID) of the plastic geomembranes and the installation quality. Due to strict quality control in Germany, both

FD and ID should be zero. However, the aging of the geomembrane will increase over time. To simulate this process, two IDs were assigned between 2051 and 2100; this is the so-called worst case. Six values are available for the installation quality of the geomembrane (perfect, excellent, good, poor, worst, and geotextile). In this investigation, the value "good" was used, i.e., good installation with a carefully prepared, smooth surface is assumed. In addition, the formation of folds in the geomembrane is controlled to achieve good contact between the geomembrane and the adjacent infiltration control layer. The soil physical input data are summarised in Table 3.

The range of the values for the soil physical data were obtained from several sources during a separate literature research, fabrication data from manufacturer data sheets and supplementary soil mechanical analysis that have been performed by the uranium mine dump operator (Table 2).

In the context of uranium mining dump capping systems, only unsaturated flow does play a role. The ground water level is not considered because: (1) uraniums mine dumps are only permitted to be located in regions of a surface far groundwater level due to risk considerations, (2) in Aue / Bad Schlema region, there is only hard rock in the underground that lacks an aquifer (which complies with the requirement of having low or unpermeable materials in the underground). There is a small weathering zone on the hard rocks that might temporarily contain pore water, but not fulfilling the characteristics of an aquifer.

3. Result

3.1. Climate variables

The temporal trends of four selected climatic variables—temperature, precipitation, global radiation, and relative humidity—were analyzed across the four quarters of the year. The results showed a consistent upward trend in mean temperature across all quarters, with significant warming observed over the study period. Precipitation patterns revealed a marked decrease during the third quarter, while an increase was observed in both the second and fourth quarters. Global radiation exhibited relatively stable values throughout the year, with no significant differences detected between quarters. In contrast, mean relative humidity showed a notable decline, particularly in the second and third quarters, under both the RCP 4.5 and RCP 8.5 emission scenarios (Fig. 2).

The statistical distribution of the temperature and the precipitation data can be seen from Fig. 3. While the annual mean temperature data show an upward trend, this is not the case for the precipitation data.

Mean temperatures are expected to rise significantly through the 21st century, with the magnitude of warming closely tied to greenhouse gas emission levels. Higher emission scenarios not only result in more warming but also increased variability, which could imply greater risk for extreme weather and climate events. From a historical mean of 7.21 °C (1999–2020), annual mean temperatures are projected to increase across all future climate scenarios: RCP 2.6: 8.96 °C (+1.75 °C), RCP 4.5: 9.53 °C (+2.32 °C), and RCP 8.5: 10.67 °C (+3.46 °C). This reinforces that higher emissions correlate with greater warming. The historical mean temperature (1999–2020) was 7.21 °C, with a small standard deviation (0.68 °C), indicating relatively stable temperature conditions. Under all three future climate scenarios (RCP 2.6, 4.5, and 8.5), mean temperatures are projected to increase substantially by 2100.

The annual mean temperature values developed from 7.21 °C (1999–2020, SD 0.68 °C, median 7.19 °C, coefficient of determination R^2 0.4676, linear trend) to 8.96 °C for RCP 2.6 (2021–2100; SD 0.62 °C, median 9.04 °C, R^2 0.2102, polynomic trend), and to 9.53 °C for RCP 4.5 (2021–2100; SD 0.59 °C, median 9.69 °C, R^2 0.5465, polynomic trend), as well as to 10.67 °C for RCP 8.5 (2021–2100; standard deviation 1.54 °C, median 10.64 °C, R^2 0.867, exponential trend). The standard deviation (SD) increases notably under RCP 8.5 (1.54 °C) compared to the other scenarios (~0.6 °C), suggesting greater variability and uncertainty in future temperatures under high-emission pathways. The median values closely align with the means in all cases, indicating symmetrical distributions of the temperature projections. Standard deviation (SD) is largest for RCP 8.5 (1.54 °C), indicating greater variability and uncertainty—possibly due to extreme events or feedbacks in a warmer climate. Lower SDs under RCP 2.6 and 4.5 suggest more climatic stability under mitigated emission pathways.

The R^2 of the historical data (1999–2020) show a moderate linear warming over the past two decades, while for RCP 2.6 was concluded a weak fit, and future temperatures fluctuate modestly and the warming stabilizes toward the end of the century (consistent with aggressive mitigation). The R^2 of the RCP 4.5 shows a moderate fit, indicating that warming continues non-linearly, likely plateauing in later decades. Finally, the data for RCP 8.5 show a strong fit, thus future temperatures are projected to increase rapidly and non-linearly, highlighting accelerated warming under high-emission scenarios.

The data demonstrates a clear link between emissions and temperature increases, not just in magnitude but also in pattern and variability. The high R^2 value and exponential trend for RCP 8.5 suggest a very strong and accelerating warming signal, which is concerning from a

Table 1
Geographical and vegetation characteristics of the model dump and characteristics of the GM over the period under consideration.

Category	Parameter	Zero model	Current state 1	Current state 2	Recultivation type 1	Recultivation type 2
Case	Case	No cover	single-layer covering	two-layer cover	A1, A3, B1, B3	A2, A4, B2, B4
Geographically	Area	25 ha	25 ha	25 ha	25 ha	25 ha
	slope inclination	24.20 %	24.20 %	24.20 %	24.20 %	24.20 %
	slope length	101.9 m	101.9 m	101.9 m	101.9 m	101.9 m
	drainage layer inclination	5 %	5 %	5 %	5 %	5 %
	drainage layer length	100 m	100 m	100 m	100 m	100 m
vegetation	vegetation	No	grass	grass	grass	trees
	topsoil	0 cm	20 cm	45 cm	20 cm	30 cm
	underbody	0 cm	80 cm	45 cm	80 cm	270 cm
	rooting depth	20 cm	100 cm	100 cm	100 cm	250 cm
	leaf area index	0	5	5	5	7
	coverage line	-	moderate	moderate	moderate	excellent
	number of curves (calculated automatically)	20 (predefined)	71.15	71.15	71.15	59.27
sealing elements	installation quality	-	-	-	good	good
	manufacturing defect density	-	-	-	0	0
	installation defect density_1999–2020	-	-	-	0	0
	installation defect density_2021–2050	-	-	-	0	0
	Installation defect density_2051–2100_Normal	-	-	-	0	0
	Installation defect density_2051–2100_Worst	-	-	-	2	2

Table 2
Overview on the literature research data for the soil physical input data.

Type of material	Pore volume [vol/vol]	Usable field capacity [vol /vol]	Wilting point [vol/vol]	Hydraulic conductivity [cm/s]	Rooting depth [cm]	source
Upper recultivation soil	0.35–0.55	> 0.15 (up to 0.25, min. 0.14)	0.15 up to 0.25	$1*10^{-3}$ to $1*10^{-6}$	Up to 30	[37–42]
Lower recultivation soil	0.30–0.45	> 0.25 (up to 0.35, min. 0.14)	0.15 up to 0.25	$1*10^{-2}$ to $1*10^{-4}$	bis 100 cm	[37–42]
Plastic drain element (PDE)	0.40	0.06	0.02	500–60	-	[43]
geomembrane (GM)	-	-	-	$2*10^{-11}$	-	[44–48]
Dump material	0.30	0.03 up to 0.10	0.04	$5*10^{-1}$ to $1*10^{-3}$	-	[37–41, 49]
Separation textile 300 g/m²	0.40	0.04	0.02	1	-	[50, 51]
Mineral drainage 16/32	0.39	0.40	0.13	1	-	[52]
Protection textile 1.200 g/m²	0.40	0.04	0.02	1	-	[50, 51]
Asphalt sealing layer	≤ 0.03	-	-	$1*10^{-15}$	-	[45,53–56]
Asphalt base layer	≤ 0.03	-	-	$1*10^{-11}$	-	[45, 53–56]

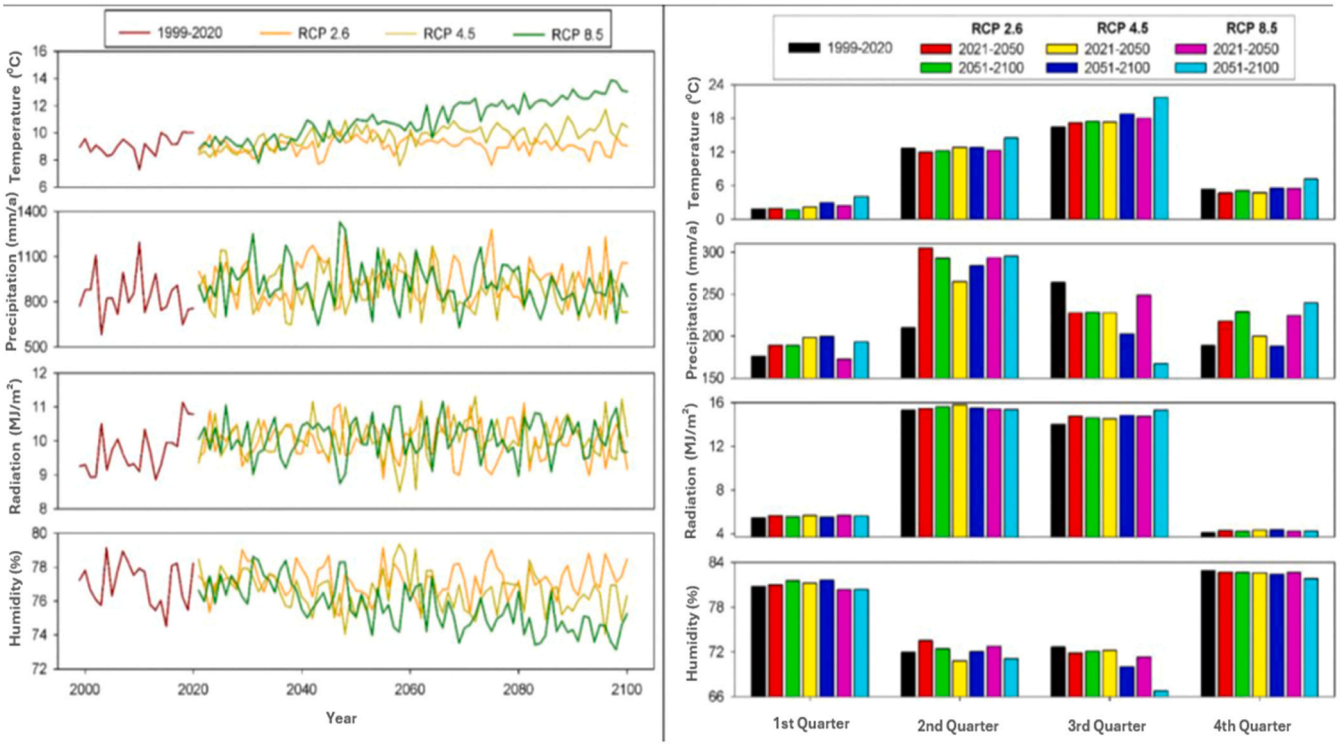

Fig. 2. Temporal patterns of four climatic variables between 1999 and 2100 under three emission scenarios (left) and comparisons of four climatic variables in the quarter between seven periods (right).

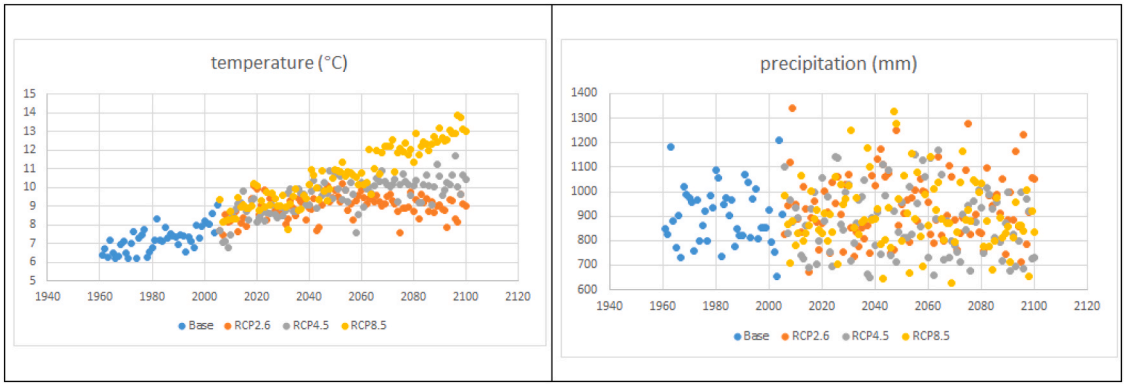

Fig. 3. Statistical distribution of temperature and precipitation data between 1999 and 2100 under three emission scenarios.

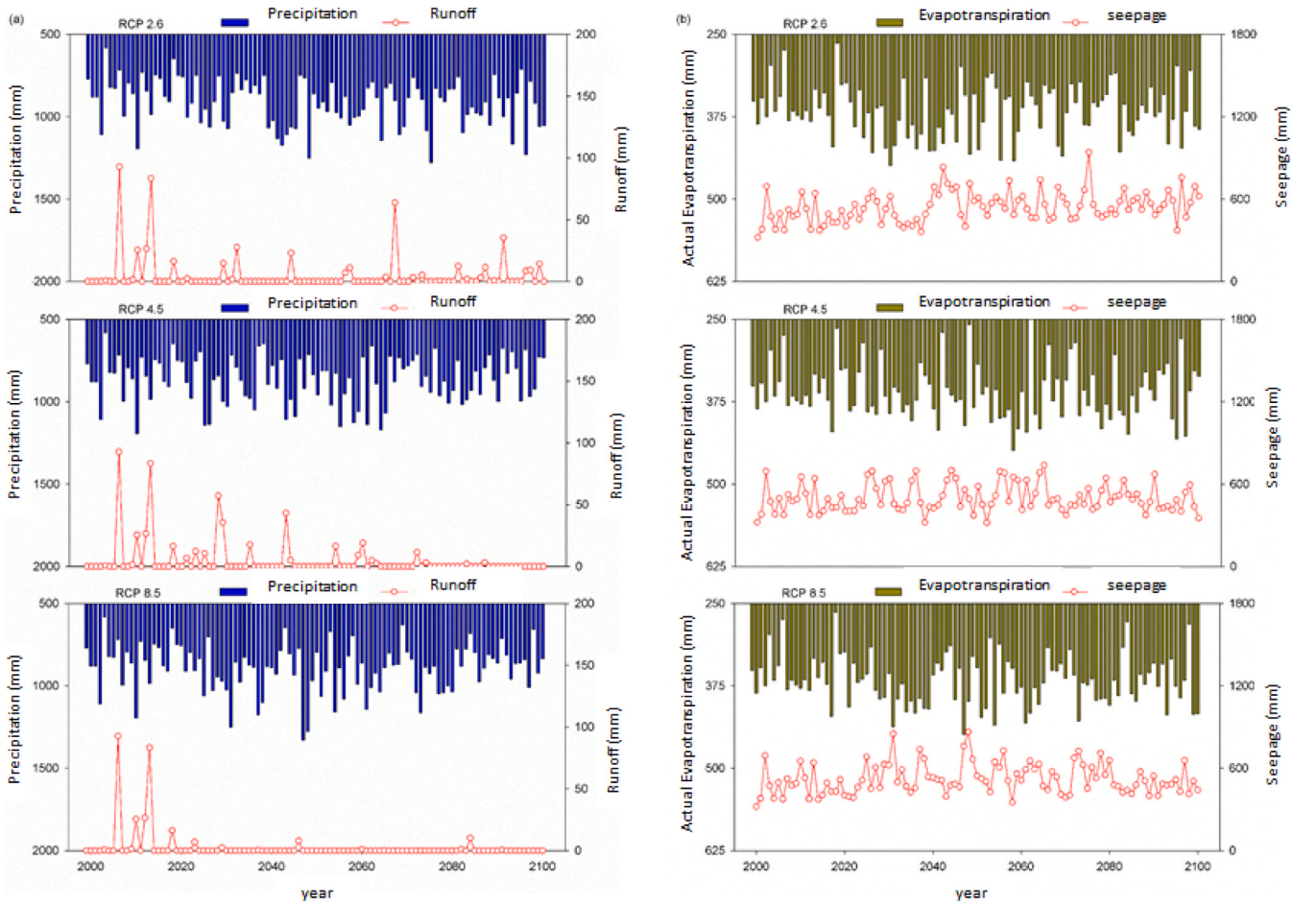

Fig. 4. Modeling results for the reference model (no cover).

climate risk perspective. The weaker R^2 and polynomial trend under RCP 2.6 suggest that intensive mitigation can stabilize temperatures, albeit with some short-term variability.

Unlike temperature, precipitation projections do not show a consistent increase or decrease: Historical (1999–2020): Mean = 901.7 mm, Median = 903.8 mm; RCP 2.6: Mean = 936.6 mm (↑ +34.9 mm), RCP 4.5: Mean = 878.8 mm (↓ −22.9 mm), and RCP 8.5: Mean = 910.4 mm (↑ +8.7 mm). This suggests no robust directional change in annual precipitation across scenarios. No meaningful trend in annual precipitation is evident in the historical record or projections under RCP scenarios. Interannual variability remains high, and future precipitation patterns may be more influenced by extreme events or regional weather systems than by a consistent long-term trend. Even with different emissions scenarios, the precipitation response is weak and inconsistent, unlike the much clearer patterns seen in temperature data. Year-to-year variability dominates over any long-term trend, which is common in precipitation datasets due to the complexity of hydrological and atmospheric systems.

The annual mean precipitation values developed from 901.7 mm (1999–2020, standard deviation 119.2 mm, median 903.8 mm, R^2 0.0102, polynomic trend) to 936.6 mm for RCP 2.6 (2021–2100; standard deviation 137.4 mm, median 910.4 mm, R^2 0.003, polynomic trend), and to 878.8 mm for RCP 4.5 (2021–2100; standard deviation 137.2 mm, median 873.8 mm, R^2 0.0272, polynomic trend), as well as to 910.4 mm for RCP 8.5 (2021–2100; standard deviation 137.2 mm, median 884 mm, R^2 0.0593, polynomic trend). Median values stay relatively close to the means, suggesting symmetrical distributions and no significant skew in projections. However, under RCP 8.5, the mean (910.4 mm) is noticeably higher than the median (884 mm), hinting at a potential skew toward wetter years or occasional extreme precipitation events. No strong trend toward wetter or drier annual conditions is evident across scenarios. RCP 2.6 shows a modest increase in mean precipitation. RCP 4.5 shows a slight decrease, and RCP 8.5 a slight increase, but differences are relatively small. However, all scenarios point to greater interannual variability, which could mean more frequent dry or wet years, increasing the risk of droughts and floods even if the long-term mean remains similar.

3.2. *Model calibration and validation*

Before analyzing the different sealing scenarios, model calibration was carried out using historical climate data from 1999 to 2020. The observed precipitation, air temperature, and solar radiation values, sourced from the German Weather Service (DWD), were used as input for the HELP model. Calibration focused on a sensitivity analysis optimizing key parameters, including soil properties (e.g., field capacity, hydraulic conductivity) and material properties for each cover configuration.

Because this study focuses on forward-looking scenario simulations using the HELP model, real-world calibration using monitoring data from implemented sealing systems was not possible. The simulations were conducted using validated hydrological and material parameters derived from previous studies and technical specifications relevant to landfill and waste containment systems. While the HELP model has been validated in numerous contexts for water balance prediction, sensitivity analyses were conducted in this study to test model stability and performance under a range of climatic and hydraulic scenarios. This approach ensures internal consistency and helps identify the range of

possible system behaviors. Future monitoring data from uranium heap remediation projects may allow retrospective validation and calibration of the modeled systems.

3.3. Performance of sealing scenarios

3.3.1. Overview

The simulation results were calculated for each of the 11 modeled

Table 3
Soil physical input data.

variant		layer	layer type	thickness (cm)	pore volume (vol/vol)	field capacity (vol/vol)	wilting point (vol/vol)	Kf-value (cm/s)
Null model	1	dump material	VPL: Vertical percolation layer	1500	0.3	0.065	0.04	2.00E−02
reference state 1	1	upper recultivation layer	VPL: Vertical percolation layer	20	0.45	0.3	0.2	1.00E−03
	2	lower recultivation layer	VPL: Vertical percolation layer	80	0.375	0.21	0.2	2.75E−04
	3	dump material	VPL: Vertical percolation layer	1500	0.3	0.065	0.04	2.00E−02
reference state 2	1	upper recultivation layer	VPL: Vertical percolation layer	45	0.31435	0.2831	0.11795	3.70E−03
	2	lower recultivation layer	VPL: Vertical percolation layer	45	0.3132	0.26365	0.12785	4.39E−04
	3	dump material	VPL: Vertical percolation layer	1500	0.3	0.065	0.04	2.00E−02
A1	1	upper recultivation layer	VPL: Vertical percolation layer	20	0.45	0.3	0.2	1.00E−03
	2	lower recultivation layer	VPL: Vertical percolation layer	80	0.375	0.21	0.2	2.75E−04
	3	PDE	LDL: Lateral drainage layer	8	0.4	0.06	0.02	1.00E+ 01
	4	GM	GML:Geomembrane	2.5	-	-	-	2.00E−11
	5	dump material	VPL: Vertical percolation layer	1500	0.3	0.065	0.04	2.00E−02
A2	1	upper recultivation layer	VPL: Vertical percolation layer	30	0.45	0.3	0.2	1.00E−03
	2	lower recultivation layer	VPL: Vertical percolation layer	270	0.375	0.21	0.2	2.75E−04
	3	PDE	LDL: Lateral drainage layer	8	0.4	0.06	0.02	1.00E+ 01
	4	GM	GML:Geomembrane	2.5	-	-	-	2.00E−11
	5	dump material	VPL: Vertical percolation layer	1500	0.3	0.065	0.04	2.00E−02
A3	1	upper recultivation layer	VPL: Vertical percolation layer	20	0.45	0.3	0.2	1.00E−03
	2	lower recultivation layer	VPL: Vertical percolation layer	80	0.375	0.21	0.2	2.75E−04
	3	separation textile 300 g/m2	LDL: Lateral percolation layer	0.3	0.4	0.04	0.02	1.00E+ 00
	4	mineral drainage	LDL: Lateral percolation layer	30	0.39	0.3	0.13	1.00E+ 00
	5	protection textile 1200 g/m2	LDL: Lateral percolation layer	0.8	0.4	0.04	0.02	1.00E+ 00
	6	GM	GML:Geomembrane	2.5	-	-	-	2.00E−11
	7	dump material	VPL: Vertical percolation layer	1500	0.3	0.065	0.04	2.00E−02
A4	1	upper recultivation layer	VPL: Vertical percolation layer	30	0.45	0.3	0.2	1.00E−03
	2	lower recultivation layer	VPL: Vertical percolation layer	270	0.375	0.21	0.2	2.75E−04
	3	separation textile 300 g/m2	LDL: Lateral percolation layer	0.3	0.4	0.04	0.02	1.00E+ 00
	4	mineral drainage	LDL: Lateral percolation layer	30	0.39	0.3	0.13	1.00E+ 00
	5	protection textile 1200 g/m2	LDL: Lateral percolation layer	0.8	0.4	0.04	0.02	1.00E+ 00
	6	GM	GML:Geomembrane	2.5	-	-	-	2.00E−11
	7	dump material	VPL: Vertical percolation layer	1500	0.3	0.065	0.04	2.00E−02
B1	1	upper recultivation layer	VPL: Vertical percolation layer	20	0.45	0.3	0.2	1.00E−03
	2	lower recultivation layer	VPL: Vertical percolation layer	80	0.375	0.21	0.2	2.75E−04
	3	PDE	LDL: Lateral drainage layer	8	0.4	0.06	0.02	1.00E+ 01
	4	asphalt sealing	GML:Geomembrane	4	-	-	-	1.00E−15
	5	asphalt base layer	VPL: Vertical percolation layer	6	0.01	0.0011	0.001	1.00E−11
	6	dump material	VPL: Vertical percolation layer	1500	0.3	0.065	0.04	2.00E−02
B2	1	upper recultivation layer	VPL: Vertical percolation layer	30	0.45	0.3	0.2	1.00E−03
	2	lower recultivation layer	VPL: Vertical percolation layer	270	0.375	0.21	0.2	2.75E−04
	3	PDE	LDL: Lateral drainage layer	8	0.4	0.06	0.02	1.00E+ 01
	4	asphalt sealing	GML:Geomembrane	4				1.00E−15
	5	asphalt base layer	VPL: Vertical percolation layer	6	-	-	-	1.00E−11
	6	dump material	VPL: Vertical percolation layer	1500	0.3	0.065	0.04	2.00E−02
B3	1	upper recultivation layer	VPL: Vertical percolation layer	20	0.45	0.3	0.2	1.00E−03
	2	lower recultivation layer	VPL: Vertical percolation layer	80	0.375	0.21	0.2	2.75E−04
	3	separation textile 300 g/m2	LDL: Lateral drainage layer	0.3	0.4	0.06	0.02	1.00E+ 00
	4	mineral drainage	LDL: Lateral drainage layer	30	0.39	0.3	0.13	1.00E+ 00
	5	asphalt sealing	GML:Geomembrane	4	-	-	-	1.00E−15
	6	asphalt base layer	VPL: Vertical percolation layer	6	0.01	0.0011	0.001	1.00E−11
	7	dump material	VPL: Vertical percolation layer	1500	0.3	0.065	0.04	2.00E−02
B4	1	upper recultivation layer	VPL: Vertical percolation layer	30	0.45	0.3	0.2	1.00E−03
	2	lower recultivation layer	VPL: Vertical percolation layer	270	0.375	0.21	0.2	2.75E−04
	3	separation textile 300 g/m2	LDL: Lateral drainage layer	0.3	0.4	0.04	0.02	1.00E+ 00
	4	mineral drainage	LDL: Lateral drainage layer	30	0.39	0.3	0.13	1.00E+ 00
	5	asphalt sealing	GML:Geomembrane	4	-	-	-	1.00E−15
	6	asphalt base layer	VPL: Vertical percolation layer	6	0.01	0.0011	0.001	1.00E−11
	7	dump material	VPL: Vertical percolation layer	1500	0.3	0.065	0.04	2.00E−02

scenarios across three timeframes: 1999–2020, 2021–2050, and 2051–2100. The water balance dynamics for each sealing configuration were assessed under current and projected climate conditions, including variations in manufacturing defect density (MDD) and installation defect density (IDD). As shown in Table 4, infiltration rates increased as the surface runoff decreased in all variants, despite higher annual runoff volumes under RCP 8.5. This is due to the high permeability of layers in the null state. Additionally, it should be noted that the HELP model has low sensitivity to surface runoff values below 10 mm. The performance of the sealing systems is represented through the seepage values, thus the potential leakage through the sealing element. For the system without sealing (reference state) the seepage value represents the pore water flow through the dump material.

As shown in Table 4, infiltration rates increased as surface runoff decreased across all variants, despite higher annual runoff volumes under the RCP 8.5 emission scenario. This is due to the high permeability of the layers in the null state, which allows more infiltration before runoff occurs. It's also worth noting that the HELP model exhibits low sensitivity to surface runoff values below 10 mm, which may explain some of the observed trends.

In the historical climate state, the surface runoff ranged from 11.20 mm for a dump without cover. In the single layer scenario, the surface runoff was modeled with 6.85 mm, compared to 19.20 mm for a dump setting with a dual layer cover. This indicates that the single layer allows for a higher seepage (358.89 mm) in comparison to the dual layer (253 mm). As expected, the uncovered state allows for the highest seepage (447 mm). In all climate change scenarios, the surface runoff is lower than in the historical period, with the lowest values in the RCP 8.5 scenario with the highest temperatures. For the null model, the actual evapotranspiration ranged from 251.23 to 385.63 mm, which is the lowest range compared to the scenarios with vegetation cover. The single layer scenario provides less rooting space in comparison to the dual layer cover, which is represented in the values for the actual evapotranspiration (single layer range from 437 to 460 mm, and dual layer 533–562 mm). Accordingly, higher evapotranspiration leads to lower seepage (253–378 mm in the dual system for different scenarios).

The modeling results for the water balance components in per cent are summarized in the Tables 5 and 6 for the sealing systems A and B. The values show that the water flow is mainly shared between the water balance components actual evapotranspiration and lateral drainage. The runoff values are very small, and the modeled values for the seepage of the sealing are more or less zero. The data are visualized exemplarily for the system A in the Figs. 7 and 8 in mm. However, the seepage values through the sealing layer were zero under standard conditions, and ranged between 0.2 and 0.3 mm, under worst case conditions (combination of 2 installation defects per hectare GM and wet years). For the asphalt sealing was observed a similar situation, even the worst case was assumed for the combination of altering asphalt and wet years.

In general, surface runoff and actual evaporation remained consistent across both sealing scenarios A and B. However, leakage values were zero in all four cases within group B, indicating effective containment. Precipitation played a crucial role in shaping the water balance behavior of the uranium waste heap dumps. Specifically, precipitation was partitioned into surface runoff, actual evaporation, drainage (in cases with a drainage layer, as seen in cover scenarios A and B), infiltration, and changes in the water reservoir. In the three comparative cases, the majority of precipitation was allocated to actual evaporation and percolation. Infiltration was slightly higher in the null model (without any cover) than in the other two scenarios. As topsoil thickness increased, infiltration decreased sharply, while surface runoff and actual evaporation both increased. This highlights the role of soil thickness in influencing water dynamics at the site.

For cover scenarios A and B, most precipitation resulted in actual evaporation and surface runoff. In all four cases within group B (asphalt sealing), infiltration through geomembranes (GM) or asphalt was zero. Similarly, in all four standard cases within group A (geomembrane covers), infiltration was effectively zero, except for minimal infiltration (0.1 %) in the worst-case scenarios A3 and A4, where small defects were considered. The results demonstrate that both sealing systems effectively reduce infiltration, surface runoff, and seepage, maintaining low infiltration rates even under worst-case scenarios, thereby ensuring long-term environmental safety.

3.3.2. *Reference model (No Cover)*

The reference model, representing a baseline with no cover or sealing, demonstrated the highest levels of leachate formation. Without sealing element, water infiltration was not controlled, leading to significant moisture movement through the waste heap pile. In such case, also radon emissions can increase significantly due to the unrestricted interaction between the waste dump material and the atmosphere. Over the 100-year simulation period, leachate formation rates were consistently high, ranging from 500 to 700 mm.

Table 4
Distribution of the amount of precipitation in the uranium waste heap dump for the Null state, current scenario 1 (single-layer cover) and current scenario 2 (dual-layer cover) in mm/a.

Value	Variant	Scenario	Period	Surface drain	Actual Evapotranspiration	Seepage
Value [mm/a]	Null model	Historical	1999–2020	11.20	351.23	447.28
		RCP 2.6	2021–2050	2.31	385.63	536.74
			2051–2100	3.83	363.59	558.11
		RCP 4.5	2021–2050	6.28	359.11	502.12
			2051–2100	1.43	365.47	493.87
		RCP 8.5	2021–2050	0.58	376.00	541.98
			2051–2100	0.26	370.48	514.64
	Current Scenario(Single layer covering)	Historical	1999–2020	6.85	442.07	358.89
		RCP 2.6	2021–2050	1.75	460.23	459.85
			2051–2100	2.48	440.48	480.37
		RCP 4.5	2021–2050	3.16	437.42	424.49
			2051–2100	1.41	437.73	421.30
		RCP 8.5	2021–2050	1.53	458.15	455.52
			2051–2100	0.69	452.61	430.60
	Current Scenario(Dual layer covering)	Historical	1999–2020	19.20	533.46	253.31
		RCP 2.6	2021–2050	8.02	547.93	365.43
			2051–2100	10.77	533.37	378.87
		RCP 4.5	2021–2050	12.03	535.35	320.09
			2051–2100	5.68	536.41	319.09
		RCP 8.5	2021–2050	8.14	557.15	351.40
			2051–2100	4.10	562.04	318.28

Table 5
Modeling results for the sealing systems A (GM).

variant	scenario	period	runoff	actual evapotranspiration	drainage	seepage sealing	seepage dump	soil storage
A1	historical	1999–2020	0.7 %	52.0 %	47.3 %	0.0 %	0.0 %	0.0 %
	RCP 2.6	2021–2050	0.1 %	48.3 %	51.6 %	0.0 %	0.0 %	0.0 %
		2051–2100	0.2 %	46.4 %	53.4 %	0.0 %	0.0 %	0.0 %
		W2051–2100	0.2 %	46.4 %	53.4 %	0.0 %	0.0 %	0.0 %
	RCP 4.5	2021–2050	0.3 %	48.6 %	51.1 %	0.0 %	0.0 %	0.0 %
		2051–2100	0.1 %	49.7 %	50.2 %	0.0 %	0.0 %	0.0 %
		W2051–2100	0.1 %	49.7 %	50.2 %	0.0 %	0.0 %	0.0 %
	RCP 8.5	2021–2050	0.1 %	48.1 %	51.9 %	0.0 %	0.0 %	0.0 %
		2051–2100	0.0 %	50.1 %	49.9 %	0.0 %	0.0 %	0.0 %
		W2051–2100	0.0 %	50.1 %	49.8 %	0.0 %	0.0 %	0.0 %
A2	Historisch	1999–2020	0.4 %	57.5 %	42.1 %	0.0 %	0.0 %	0.0 %
	RCP 2.6	2021–2050	0.1 %	53.0 %	46.9 %	0.0 %	0.0 %	0.0 %
		2051–2100	0.1 %	51.3 %	48.6 %	0.0 %	0.0 %	0.0 %
		W2051–2100	0.1 %	51.3 %	48.6 %	0.0 %	0.0 %	0.0 %
	RCP 4.5	2021–2050	0.2 %	53.9 %	45.9 %	0.0 %	0.0 %	0.0 %
		2051–2100	0.1 %	54.6 %	45.3 %	0.0 %	0.0 %	0.0 %
		W2051–2100	0.1 %	54.6 %	45.2 %	0.0 %	0.0 %	0.0 %
	RCP 8.5	2021–2050	0.0 %	53.5 %	46.5 %	0.0 %	0.0 %	0.0 %
		2051–2100	0.0 %	55.2 %	44.8 %	0.0 %	0.0 %	0.0 %
		W2051–2100	0.0 %	55.2 %	44.8 %	0.0 %	0.0 %	0.0 %
A3	historical	1999–2020	0.8 %	52.7 %	46.5 %	0.0 %	0.0 %	0.0 %
	RCP 2.6	2021–2050	0.2 %	48.9 %	50.9 %	0.0 %	0.0 %	0.0 %
		2051–2100	0.3 %	46.9 %	53.0 %	0.0 %	0.0 %	−0.1 %
		W2051–2100	0.3 %	46.9 %	52.8 %	0.1 %	0.1 %	0.0 %
	RCP 4.5	2021–2050	0.4 %	49.1 %	50.4 %	0.0 %	0.0 %	0.1 %
		2051–2100	0.2 %	50.1 %	49.7 %	0.0 %	0.0 %	0.0 %
		W2051–2100	0.2 %	50.1 %	49.5 %	0.1 %	0.1 %	0.1 %
	RCP 8.5	2021–2050	0.2 %	48.8 %	51.0 %	0.0 %	0.0 %	0.0 %
		2051–2100	0.1 %	50.6 %	49.3 %	0.0 %	0.0 %	0.0 %
		W2051–2100	0.1 %	50.6 %	49.2 %	0.1 %	0.1 %	0.0 %
A4	historical	1999–2020	0.4 %	57.0 %	42.6 %	0.0 %	0.0 %	0.0 %
	RCP 2.6	2021–2050	0.1 %	52.9 %	47.0 %	0.0 %	0.0 %	0.0 %
		2051–2100	0.1 %	51.2 %	48.7 %	0.0 %	0.0 %	0.0 %
		W2051–2100	0.1 %	51.2 %	48.6 %	0.1 %	0.1 %	0.0 %
	RCP 4.5	2021–2050	0.2 %	53.9 %	45.9 %	0.0 %	0.0 %	0.0 %
		2051–2100	0.1 %	54.6 %	45.3 %	0.0 %	0.0 %	0.0 %
		W2051–2100	0.1 %	54.6 %	45.2 %	0.1 %	0.1 %	0.0 %
	RCP 8.5	2021–2050	0.0 %	53.5 %	46.5 %	0.0 %	0.0 %	0.0 %
		2051–2100	0.0 %	55.1 %	44.9 %	0.0 %	0.0 %	0.0 %
		W2051–2100	0.0 %	55.1 %	44.8 %	0.1 %	0.1 %	0.0 %

3.3.3. *Current State 1 (Single-Layer Cover)*

The single-layer cover (Current State 1), typical of the waste pile configuration in Aue, showed moderate improvements compared to the reference model, seepage ranging from 250 to 600 mm. While leachate formation was somewhat reduced, the sealing effectiveness against radon exhalation was considered to be insufficient, as it is observed in the present situation at this location.

3.3.4. *Current State 2 (Dual-Layer Cover)*

The dual-layer cover, as seen for instance at the Königstein uranium dump site, performed better in terms of reducing both leachate formation and radon emissions. The additional layer improved the water retention capacity and reduced the permeability of the cover. During the 2021–2050 period, with moderate climate changes, leachate rates were significantly lower compared to Current State 1, ranging from 50 to 500 mm, with peaks up to 800 mm. However, in the worst-case scenario for 2051–2100, the performance of the two-layer cover was diminished due to the potential for localized degradation of the cover system, especially in the upper soil layers.

3.3.5. *Sealing systems*

In the current state, the absence of sealing elements resulted in a water balance characterized by high infiltration levels into the slag heap body. Without a cover, over half of the precipitation infiltrated into the waste pile, and this trend was expected to persist in the future if the site remained uncovered. For the existing cover systems, the single-layer cover reduced seepage by approximately 100 mm annually, while the dual-layer system reduced seepage by about 200 mm annually compared to the uncovered state.

The simulation results also showed an upward trend in evaporation after 2050, attributed to anticipated increases in annual mean temperatures. Interestingly, in the current state (without a cover or with a mineral cover lacking sealing elements), infiltration slightly exceeded evaporation, primarily due to the high permeability of the waste pile. This facilitated greater infiltration, a pattern that extended to existing cover systems without sealing elements, where differences in hydraulic conductivity (Kf) values created a hydraulic gradient, allowing water to infiltrate the waste heap pile.

As anticipated, simulations with waterproofing systems (either geomembranes or asphalt seals) yielded near-zero infiltration rates. Under both current and forecasted climate conditions, infiltration remained effectively zero under typical scenarios without leaks in the sealing element, rendering the system convection-tight and preventing radon from migrating through the sealing layers.

Figs. 7 and 8 illustrate the evolution of actual evaporation and seepage over time. For the worst-case scenarios (A1-A4), seepage through the geomembrane (GM) remained relatively constant over time, with slightly higher levels under the RCP 2.6 scenario. In the worst-case scenarios A1 and A2 (Fig. 7), seepage through the waste pile body increased slightly during the first half of the period (2051–2100) and more rapidly in the second half, due to the assumption of damage to the sealing element. For the worst-case scenarios A3 and A4, this increase in seepage occurred earlier, around 2057, due to the assumed defects in the sealing layer. The system reached an equilibrium point by 2065 (Fig. 8).

Overall, the surface runoff and actual evaporation values were identical between cases A and B, and the infiltration values approached

Table 6
Modeling results for the sealing systems B (asphalt).

variant	scenario	period	runoff	actual evapotranspiration	drainage	seepage sealing	seepage dump	soil storage
B1	historical	1999–2020	0.7 %	52.0 %	47.3 %	0.0 %	0.0 %	0.0 %
	RCP 2.6	2021–2050	0.1 %	48.3 %	51.6 %	0.0 %	0.0 %	0.0 %
		2051–2100	0.2 %	46.4 %	53.4 %	0.0 %	0.0 %	0.0 %
		W2051–2100	0.2 %	46.4 %	53.4 %	0.0 %	0.0 %	0.0 %
	RCP 4.5	2021–2050	0.3 %	48.6 %	51.1 %	0.0 %	0.0 %	0.0 %
		2051–2100	0.1 %	49.7 %	50.2 %	0.0 %	0.0 %	0.0 %
		W2051–2100	0.1 %	49.7 %	50.2 %	0.0 %	0.0 %	0.0 %
	RCP 8.5	2021–2050	0.1 %	48.1 %	51.9 %	0.0 %	0.0 %	0.0 %
		2051–2100	0.0 %	50.1 %	49.9 %	0.0 %	0.0 %	0.0 %
		W2051–2100	0.0 %	50.1 %	49.9 %	0.0 %	0.0 %	0.0 %
B2	historical	1999–2020	0.4 %	57.5 %	42.1 %	0.0 %	0.0 %	0.0 %
	RCP 2.6	2021–2050	0.1 %	53.0 %	46.9 %	0.0 %	0.0 %	0.0 %
		2051–2100	0.1 %	51.3 %	48.6 %	0.0 %	0.0 %	0.0 %
		W2051–2100	0.1 %	51.3 %	48.6 %	0.0 %	0.0 %	0.0 %
	RCP 4.5	2021–2050	0.2 %	53.9 %	45.9 %	0.0 %	0.0 %	0.0 %
		2051–2100	0.1 %	54.6 %	45.3 %	0.0 %	0.0 %	0.0 %
		W2051–2100	0.1 %	54.6 %	45.3 %	0.0 %	0.0 %	0.0 %
	RCP 8.5	2021–2050	0.0 %	53.5 %	46.5 %	0.0 %	0.0 %	0.0 %
		2051–2100	0.0 %	55.2 %	44.8 %	0.0 %	0.0 %	0.0 %
		W2051–2100	0.0 %	55.2 %	44.8 %	0.0 %	0.0 %	0.0 %
B3	historical	1999–2020	0.7 %	51.8 %	47.5 %	0.0 %	0.0 %	0.0 %
	RCP 2.6	2021–2050	0.1 %	48.1 %	51.7 %	0.0 %	0.0 %	0.0 %
		2051–2100	0.2 %	46.3 %	53.5 %	0.0 %	0.0 %	0.0 %
		W2051–2100	0.2 %	46.3 %	53.5 %	0.0 %	0.0 %	0.0 %
	RCP 4.5	2021–2050	0.3 %	48.4 %	51.3 %	0.0 %	0.0 %	0.0 %
		2051–2100	0.1 %	49.6 %	50.2 %	0.0 %	0.0 %	0.0 %
		W2051–2100	0.1 %	49.6 %	50.2 %	0.0 %	0.0 %	0.0 %
	RCP 8.5	2021–2050	0.1 %	47.9 %	52.0 %	0.0 %	0.0 %	0.0 %
		2051–2100	0.0 %	50.1 %	49.9 %	0.0 %	0.0 %	0.0 %
		W2051–2100	0.0 %	50.1 %	49.9 %	0.0 %	0.0 %	0.0 %
B4	historical	1999–2020	0.4 %	57.5 %	42.2 %	0.0 %	0.0 %	0.0 %
	RCP 2.6	2021–2050	0.1 %	53.0 %	46.9 %	0.0 %	0.0 %	0.0 %
		2051–2100	0.1 %	51.3 %	48.6 %	0.0 %	0.0 %	0.0 %
		W2051–2100	0.1 %	51.3 %	48.6 %	0.0 %	0.0 %	0.0 %
	RCP 4.5	2021–2050	0.2 %	53.9 %	45.9 %	0.0 %	0.0 %	0.0 %
		2051–2100	0.1 %	54.6 %	45.3 %	0.0 %	0.0 %	0.0 %
		W2051–2100	0.1 %	54.6 %	45.3 %	0.0 %	0.0 %	0.0 %
	RCP 8.5	2021–2050	0.0 %	53.5 %	46.5 %	0.0 %	0.0 %	0.0 %
		2051–2100	0.0 %	55.2 %	44.8 %	0.0 %	0.0 %	0.0 %
		W2051–2100	0.0 %	55.2 %	44.8 %	0.0 %	0.0 %	0.0 %

zero for all four cases of group B. Therefore, the patterns of surface runoff, actual evaporation, and infiltration were not presented for all four cases of group B. Fig. 5 shows the results of the annual data for precipitation, surface runoff, actual evaporation, and infiltration for each year from 1999 to 2100. For all 11 cases, surface runoff decreased over time, and this trend was particularly pronounced under the RCP 8.5 scenario. For the three comparison cases, there were no clear trends for actual evaporation and infiltration over time. However, infiltration was significantly higher under the worst case than under the normal cases. For the worst cases of A1-A4, the amount of infiltration through the GM remained at a similar level over time, with a higher amount under the RCP 2.6 scenario.

For the worst cases of A1 and A2, the amount of infiltration through the waste heap body increased slowly in the first half of the period 2051–2100 and rapidly in the second half of the period. The turning point was much earlier for the worst cases of A3 and A4, namely in 2057, and the values reached equilibrium in 2065. The amount of precipitation in the waste heap area can change the behavior of the waste heap's water balance. In detail, the amount of precipitation would be divided into surface runoff, actual evaporation, drainwater (only the cases of groups A and B), infiltration, and changes in the water storage. In the three comparison cases, most of the precipitation went to actual evaporation and infiltration. The amount of infiltration was relatively higher in the null model than in the other two comparison cases. With increasing topsoil thickness the amount of infiltration decreased dramatically, but the amount of surface runoff and actual evaporation increased. In cases A and B, most of the precipitation went to actual evaporation and surface runoff. With increasing topsoil thickness (i.e., recultivation type 2), the amount of runoff water decreased dramatically, but the amount of actual evaporation increased. The shares of infiltration through asphalt sealing and asphalt base layer, respectively, were zero in all four cases of B. These proportions were also zero under all four normal cases of A, and 0.1 % under the worst case of A3 and A4.

The asphalt sealing scenarios (B1–B4), using landfill-grade asphalt, also exhibited strong performance in controlling leachate formation. Similar to geomembranes, asphalt sealing was effective in reducing water infiltration and gas migration. In the 2021–2050 period, the asphalt-based covers performed comparably to the geomembrane scenarios. However, in the long term (2051–2100), asphalt seals exhibited slightly higher sensitivity to environmental aging factors. The performance of asphalt sealing layers slightly decreased in scenarios B3 and B4 due to potential cracking and permeability changes, but still remained below critical thresholds for leachate emissions.

The simulation results under different Representative Concentration Pathways (RCPs) highlighted the potential impact of climate change on sealing performance. For all sealing scenarios, rising temperatures were associated with changes in leachate dynamics. However, sealing solutions involving geomembranes (A1–A4) were significantly more resilient to these changes, maintaining a relatively stable performance even under extreme climate scenarios.

3.4. *Worst case – wet years*

To assess the impact of higher rainfall in the wet years on the infiltration of the heap, the averaged infiltration of the wettest five years was calculated for each period, and a comparison was made between the

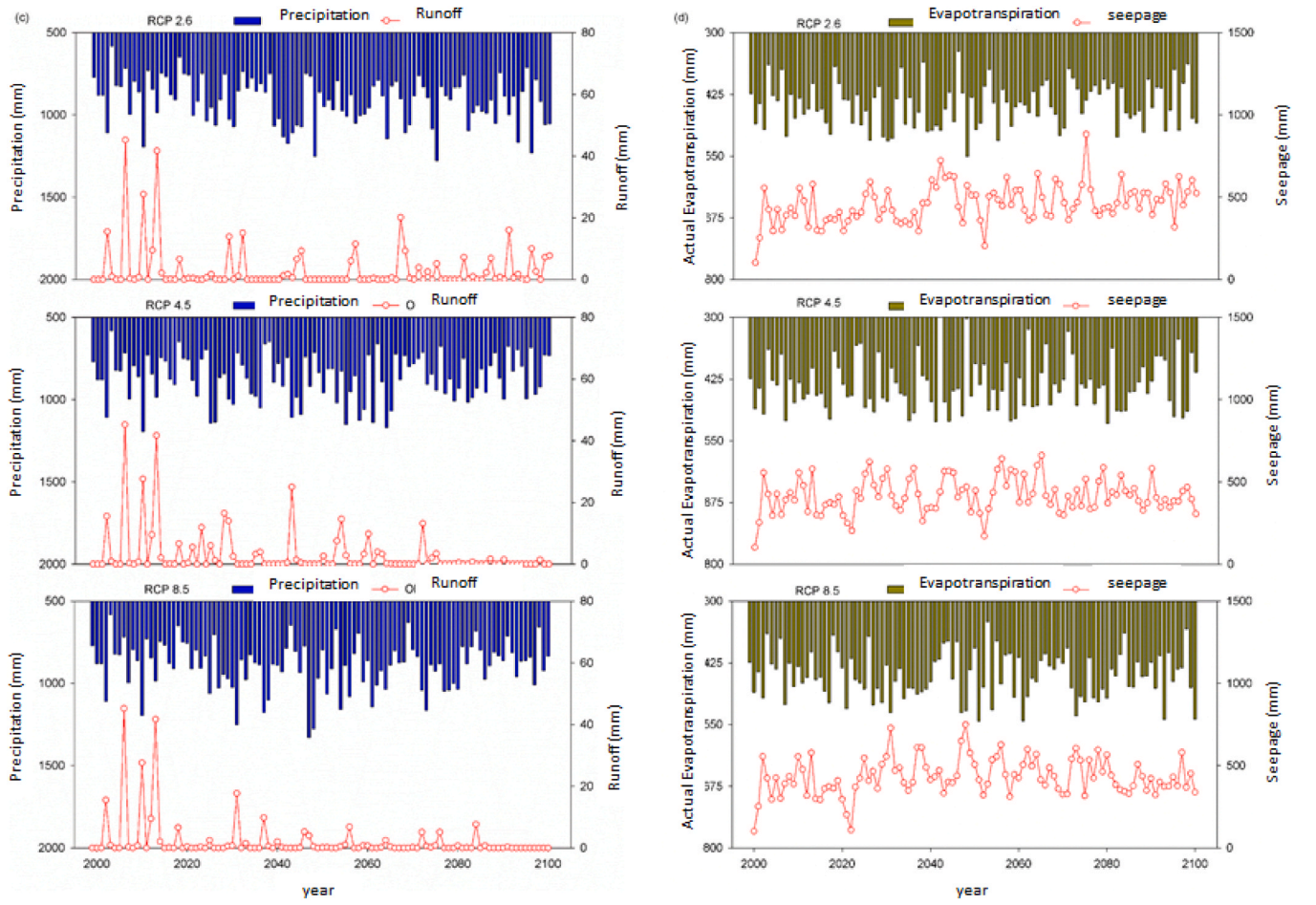

Fig. 5. Modeling results for the current state 1.

long-term annual infiltration and the averaged infiltration of the wet years. Table 7 provides a list of the five wettest years for each modelled period.

As already mentioned, the results of the precipitation prognosis showed different developments for the various climate scenarios. While the annual precipitation mean value in the period 1999–2020 was 901.7 mm, in RCP 2.6 scenario the annual mean increased by + 34.9 mm to 936.6 mm. The data for RCP 4.5 showed an annual mean decrease by −22.9 mm to 878.8 mm, and for RCP 8.5 was observed a slight increase of + 8.7 mm resulting in an annual precipitation mean of 910.4 mm. The precipitation of the wettest years ranged 909.2 to 1198.5 mm in the historical period. In the period 2021 – 2050, the highest annual precipitation means were observed under RCP 8.5, while in the period 2051 – 2100 this is was the under RCP 2.6.

The results showed that infiltration rates in the wet years were more than twice the long-term annual value under the zero model. This rate decreased with increasing topsoil thickness (Fig. 9). Due to the effect of the GM, infiltration rates through the GM approached zero under both scenarios (i.e., long-term and wet years). However, under the worst case, infiltration rates in the wet years were approximately 25 % higher than the long-term annual value. Similar patterns were also observed for leakage through the tailings pile body under the RCP 2.6 and worst-case emission scenarios. Interestingly, in the wet years, the worst-case infiltration rates were even lower than the long-term annual value under RCP 4.5 and RCP 8.5. This is because most of the wet years occurred before the inflection point (i.e., 2057) of infiltration increase under RCP 4.5 and RCP 8.5, while most of the wet years of RCP 2.6 occurred after the inflection point.

The infiltration values approached zero for all four cases of Group B. Therefore, the infiltration patterns were not presented for all four cases of Group B. The results showed that the infiltration volumes in the wet years were more than twice the long-term annual value under the zero model. This volume decreased with increasing topsoil thickness.

3.5. *Sensitivity to defects*

The worst-case scenario (2051–2100) incorporated a manufacturing defect density (MDD) of 0 and an installation defect density (IDD) of 2 per hectare. In these conditions, the results showed that the performance of all sealing systems would decline due to localized defects in the geomembrane. However, the geomembrane-based covers (A1–A4) continued to exhibit superior resilience, with minimal increases in leachate formation.

4. Discussion

The results of this study indicate that geomembrane-based sealing systems (A1–A4) provide the most reliable long-term solution for minimizing leachate formation and radon exhalation from uranium mining heaps. Asphalt-based systems (B1–B4) also offer effective sealing, though with slightly higher vulnerability to aging. The impact of climate change was found to exacerbate infiltration rates and cover degradation, but the selected sealing systems remained largely effective under projected conditions. In summary, geomembrane-based covers (A1–A4) provided the most consistent and effective sealing solution across all climate and defect scenarios. Asphalt-based covers (B1–B4) performed similarly well but showed slightly reduced long-term stability under extreme weather conditions. The dual-layer covers (Current State

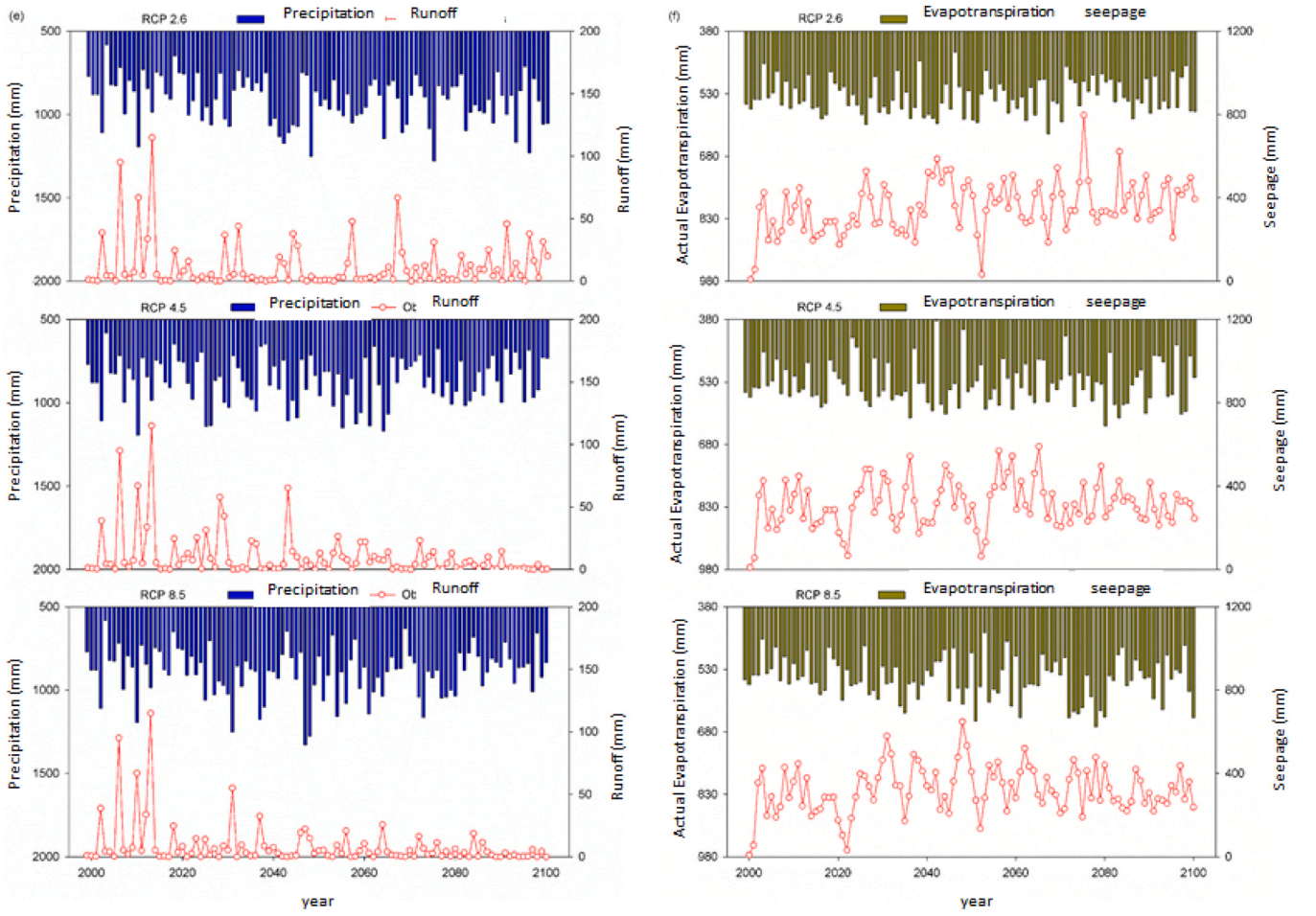

Fig. 6. Modeling results for the current state 2.

2) performed better than the single-layer covers but were not as effective as the convection-tight geomembrane or asphalt systems.

The infiltration behavior of the three comparative variants, alongside eight different sealing scenarios, was analyzed using the HELP model. This analysis incorporated both current climatic conditions and projected future climate change scenarios.

- **Uncovered State:** In the absence of a cover, the results indicated that more than half of the precipitation infiltrates into the waste heap body. This trend is expected to persist under future climate scenarios, indicating the importance of sealing systems. The application of cover systems reduced infiltration by approximately 100 mm annually for the single-layer cover and by 200 mm for the two-layer system, largely due to the increase in evaporation. These findings highlight the effectiveness of cover systems in mitigating infiltration and maintaining the stability of the waste pile.
- **Impact of Wet Years:** During particularly wet years, infiltration volumes in the uncovered state were more than double the long-term annual averages, further underscoring the vulnerability of uncovered waste heap to excessive water infiltration. However, as topsoil thickness increased, infiltration volumes decreased. In all cases with a plastic drainage element, infiltration was reduced to nearly zero, even during wet conditions. In the worst-case scenario, where leakage was assumed, infiltration during wet years was about 25 % above the long-term average, but it still remained at a low level. This suggests that while sealing elements can significantly mitigate water infiltration, extreme weather events can still lead to some additional infiltration, especially in the event of defects in the sealing layer.
- **Surface Runoff and Evaporation:** Long-term trends in surface runoff and actual evaporation were consistent across all cover scenarios (A and B). Leakage rates were zero in all four cases under cover scenario B, which highlights the robustness of the waterproofing system in preventing infiltration. Over time, surface runoff showed a decreasing trend, which is in line with expectations for a well-maintained drainage system. Interestingly, no clear trends emerged in actual evaporation and seepage rates across the three comparative variants. However, in the worst-case scenario (involving leakage), infiltration was slightly higher than in leak-free conditions, peaking at 8 mm per year. This suggests that minor defects in the sealing elements can lead to increased infiltration, but the impact remains relatively low.
- **Response to Heavy Rainfall:** The HELP model revealed that surface runoff increased immediately following heavy rainfall events, while peak infiltration rates through the waste pile were observed 3–5 days post-rainfall. This delayed response in peak infiltration is typical of systems with significant water storage capacity, such as waste piles. In cover scenario A, peak infiltration through the geomembrane (GM) occurred 1–3 days after rainfall events, but no significant increase in infiltration through the waste heap body was observed following heavy rainfall, indicating that the GM was effective in managing initial infiltration rates.
- **Seepage through the Waste Heap:** Among the sealing scenarios, asphalt sealing (cover scenarios B1 and B2) provided slightly less protection than the geomembrane sealing (scenarios A3 and A4), primarily due to the marginally lower permeability of the geomembrane. However, this difference was minimal, indicating that both types of sealing systems are highly effective in minimizing

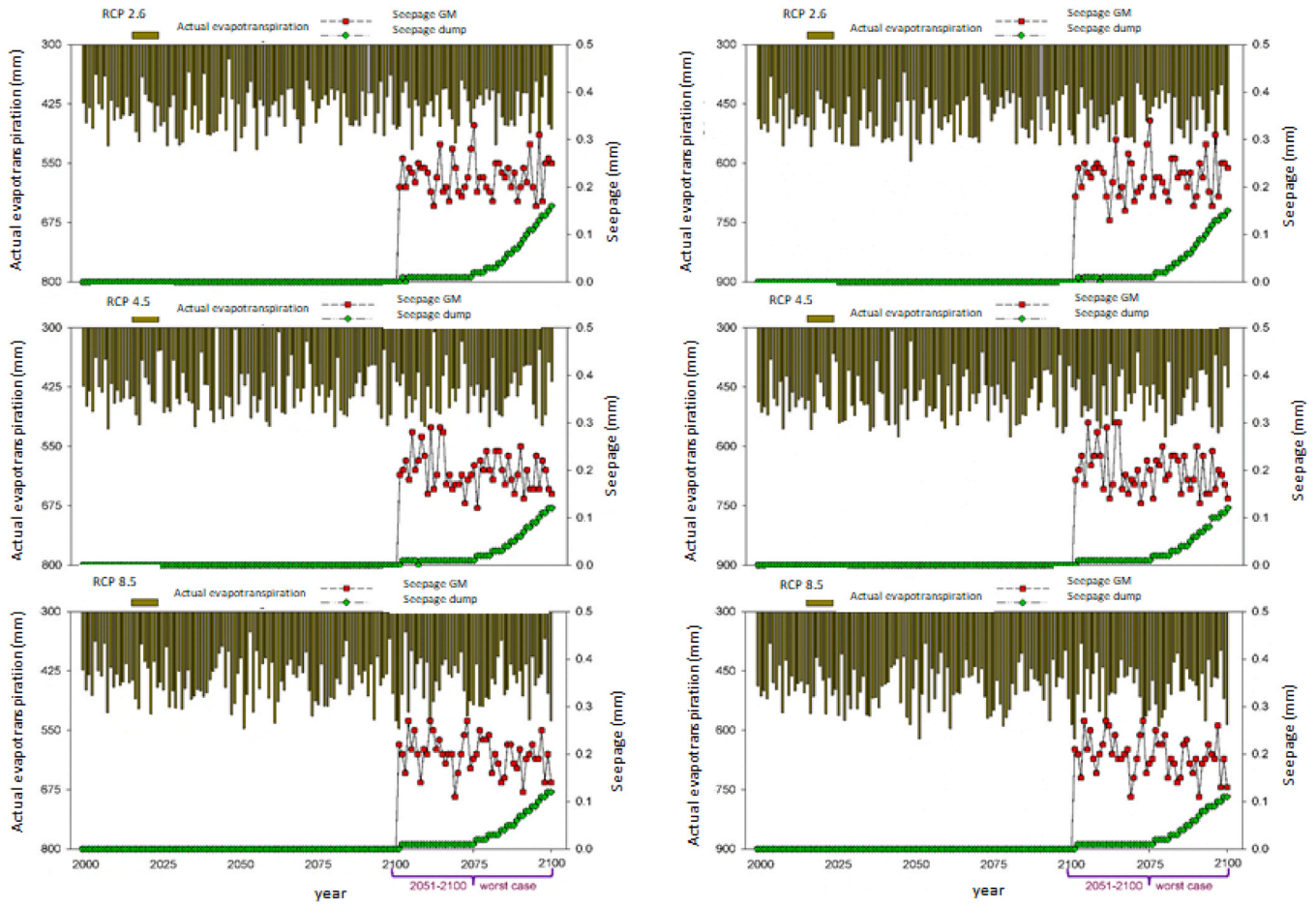

Fig. 7. Presentation of the simulation results for configuration A: actual evapotranspiration and seepage through GM and dump (A 1 and A 2).

seepage. The use of plastic drainage elements (KDE) further enhanced the performance of the sealing systems, outperforming mineral drainage in controlling seepage. From a water management perspective, cover scenarios B1 and B2 provided the most favorable outcomes, followed by scenarios A3 and A4. In all cases, except for the worst-case scenario, seepage through the sealing layers remained near zero, demonstrating the effectiveness of these cover systems in preventing water ingress.

- **Worst-Case Scenario:** In the worst-case scenario, where minor defects in the sealing elements allowed for low-level infiltration and gas permeability, the quantities of infiltration remained minimal. In scenarios A1 and A2, infiltration through the waste heap body gradually increased between 2051 and 2100, with a slightly increased rate in the latter half of the period due to the assumption of damage to the sealing element. In contrast, infiltration reached equilibrium earlier in scenarios A3 and A4, peaking around 2065. This finding underscores the importance of maintaining the integrity of sealing systems over time to minimize long-term infiltration risks.
- **Future Drought Risks:** Under future climate conditions, the risk of soil dehydration and drought significantly increased. Extreme scenarios projected a 53.9 % risk of drought, while critical scenarios suggested a 39.8 % risk. As a result, the proportion of wet soil was expected to decrease by 27.7 %. These projections highlight the potential challenges for water management and soil moisture retention in the future, emphasizing the need for robust sealing and water management strategies to mitigate these risks.

The geomembrane-based sealing scenarios (A1–A4) demonstrated the highest effectiveness in reducing leachate formation, thus also indicating an effective radon exhalation reduction. In these scenarios, the impermeable geomembrane acted as a robust barrier, effectively preventing water infiltration and gas migration. The presence of a plastic drainage layer (PDE) and recultivation soil further enhanced the performance by facilitating runoff and providing additional gas-tight protection. These geomembrane-based designs proved to be highly resilient against the effects of aging and defects, with very minimal degradation in performance over the 100-year simulation period.

The results demonstrate that both asphalt and geomembrane sealing systems are highly effective in preventing infiltration, reducing surface runoff, and ensuring radon confinement—all of which contribute to long-term environmental protection. The simulations show that, even under extreme climate scenarios, these sealing systems can prevent substantial pollution and water contamination, thus supporting the cleaner production goals of minimizing waste and conserving resources. Importantly, our findings suggest that sealing systems are resilient to climate change, as they maintain effective performance even in wet years or when subjected to increased rainfall due to climate change. By reducing the environmental footprint of historical mining waste, these systems offer a pathway toward sustainable land remediation that can be adapted to future conditions. The incorporation of climate change forecasts in this study offers valuable insights for improving policy-making and regulations related to waste management and site remediation under changing climatic conditions.

5. Conclusions

This study investigated the long-term effectiveness of asphalt and geomembrane sealing systems for uranium mining heap remediation

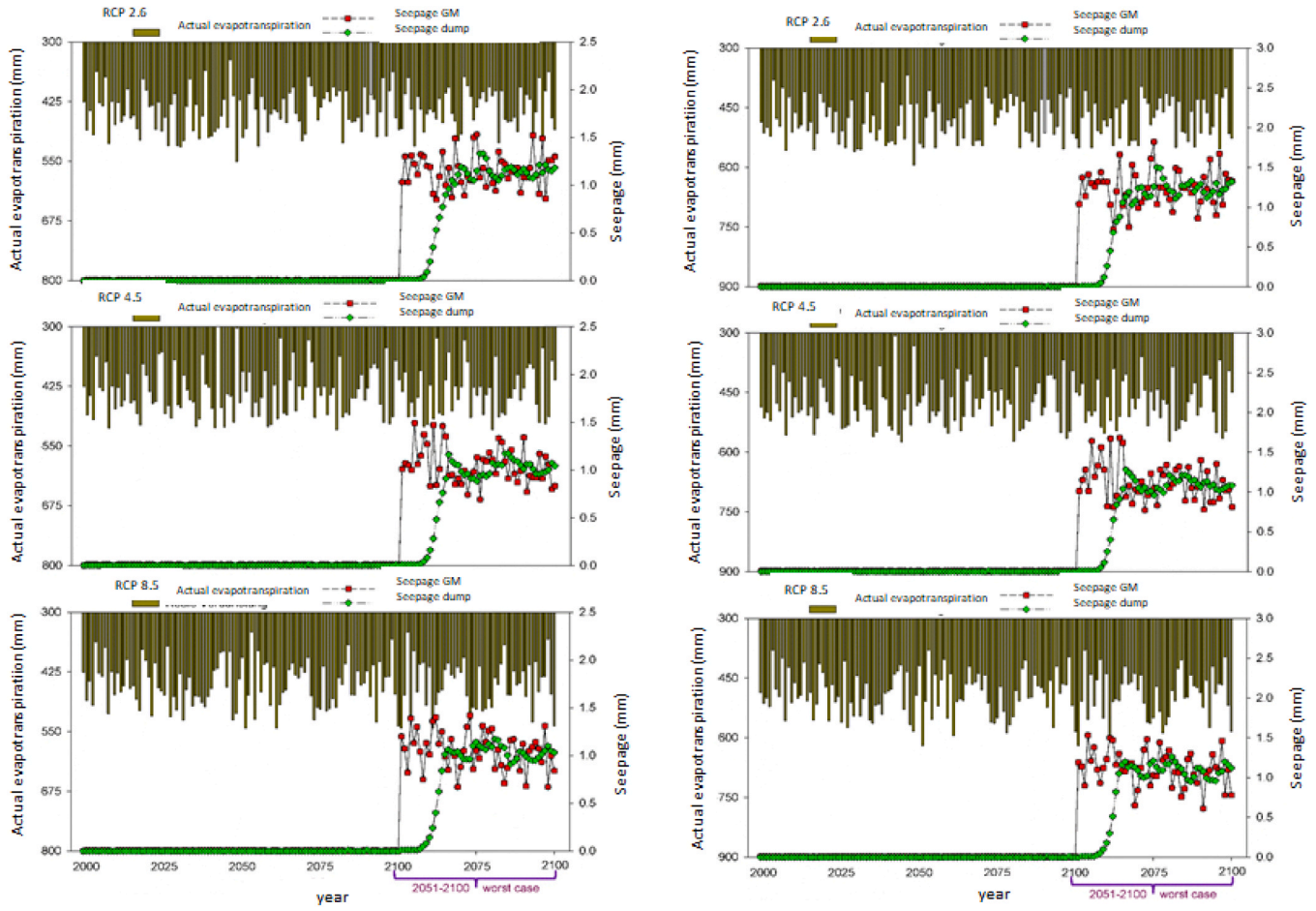

Fig. 8. Presentation of the simulation results for configuration A: actual evapotranspiration and seepage through GM and dump (A 3 and A 4).

Table 7
List of the five wettest years for each period.

Parameter	Historical	2021–2050			2051–2100		
		RCP 2.6	RCP 4.5	RCP 8.5	RCP 2.6	RCP 4.5	RCP 8.5
Year	2002	2048	2025	2047	2075	2064	2073
	2007	2042	2026	2048	2096	2055	2054
	2010	2041	2043	2031	2093	2061	2061
	2013	2043	2045	2037	2064	2058	2056
	2017	2045	2036	2038	2068	2065	2051
Precipitation	1108.6	1251.0	1142.6	1329.2	1279.0	1170.7	1163.8
	996.8	1173.9	1137.2	1277.3	1230.7	1151.0	1157.5
	1194.5	1133.3	1109.1	1251.2	1166.5	1138.9	1141.8
	985.4	1109.6	1089.9	1176.9	1144.1	1127.3	1080.2
	909.2	1072.7	1049.4	1101.5	1107.8	1069.0	1063.4

under varying climate scenarios. Using the HELP model, both systems demonstrated a high degree of impermeability, significantly reducing infiltration across all tested conditions, including extreme future climate projections. These outcomes underscore their potential to support radiation protection goals by limiting leachate generation and radon migration from uranium mine dumps.

The primary goal of appropriate sealing measures is to minimize convective radon transport from the tailings pile. The diffusive component, in contrast, generally plays only a minor role. When planning the surface sealing of the tailings pile, a target value must be specified to which the annual average radon concentration at the reference point is to be reduced. To achieve an additional effective annual dose of 1 mSv caused by the tailings pile, with an exposure duration of 7000 h/a and an equilibrium factor of 0.4, the annual average radon activity concentration outdoors is approximately 50 Bq/m^3 in addition to the natural subsurface. The increased radon concentration at the toe of the tailings pile caused by mining tailings is determined by the exhalation rate, particularly in summer, since the temperature gradient between the tailings pile and the outside air is reversed in winter, and the radon-containing pore air then flows out preferentially onto the tailings pile plateau. It can be assumed that radon exhalation is zero during the guaranteed service life of the systems on dumps that are properly sealed with GM or asphalt sealing systems.

While radon exhalation was not modeled directly, the established link between moisture flow and gas diffusion supports the inference that reducing infiltration through these sealing layers contributes to lower radon emissions. This reinforces the relevance of these systems not only for hydraulic containment but also for long-term radiological safety.

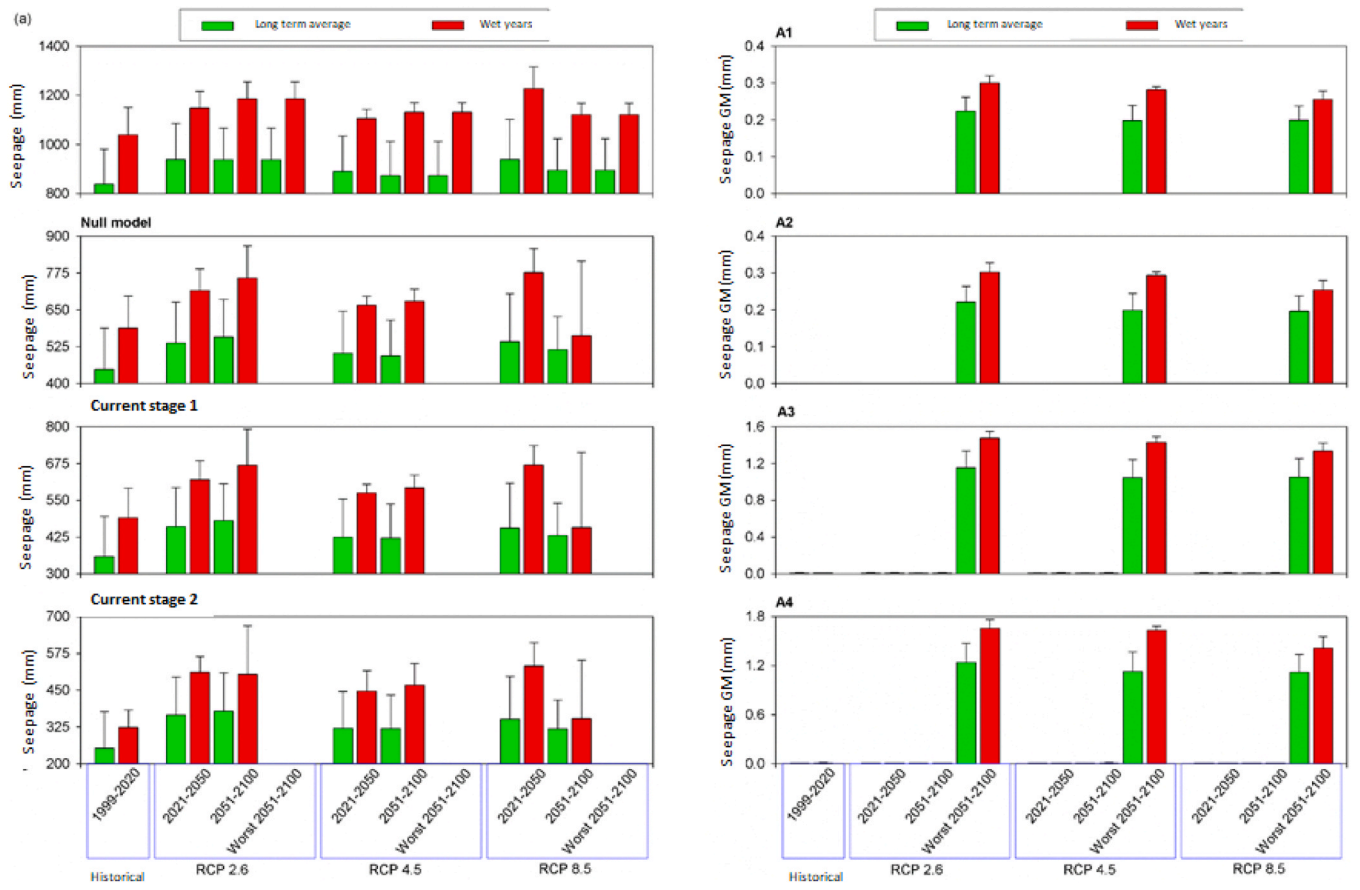

Fig. 9. Comparisons of (a) infiltration through the dump for the null model, the current state 1, and current state 2; as well as infiltration through (b) the GM for all A variants.

The main results of the water balance model calculations for sealing scenarios A and B on the model dump indicated that, up until 2050, approximately half of the precipitation was lost through evaporation, while the other half was directed to discharge within the drainage layer. After 2050, evaporation levels continued to rise, resulting in a decrease in drainage volume within the drainage element. In the baseline scenario (i.e., without defects in the sealing elements), infiltration remained negligible, confirming that the sealing layers effectively prevented seepage. This condition changed only slightly when the "worst-case" scenario, involving defects in the waterproofing element, was considered in the long-term assessment. Even in this worst-case scenario, infiltration was limited to a maximum of 8 mm beneath the geomembrane, which is still regarded as an extremely low infiltration rate.

One of the clear advantages of these synthetic sealing systems is their resistance to desiccation and physical degradation. Unlike mineral covers, which can crack under prolonged dry conditions, both asphalt and geomembrane layers remained stable throughout the simulation period. Among the two, asphalt exhibited slightly greater resilience in erosion-prone or vegetation-depleted conditions due to its greater mechanical thickness and structural robustness.

Some uncertainty remains regarding how these materials perform over extended timescales, particularly under site-specific stresses and climate variability. Field-based monitoring, validation of model outputs, and aging studies are needed to strengthen confidence in their long-term behavior. Additionally, the integration of recycled industrial by-products into sealing systems could offer improvements in sustainability and cost efficiency. Overall, the findings contribute valuable insight to the selection and design of remediation strategies at legacy uranium sites. By evaluating the hydraulic and physical performance of two proven sealing systems under climate-adaptive scenarios, this research supports more robust, informed decision-making for long-term environmental protection and sustainable site management.

Environmental Implications

The findings of this study highlight the significant environmental benefits of using asphalt and geomembrane sealing systems in the remediation of uranium mining sites. By effectively minimizing water infiltration and reducing radon emissions, these systems offer a sustainable solution that enhances long-term environmental safety. The research contributes to improving remediation strategies, ensuring better water management, mitigating climate change impacts, and supporting environmental protection in uranium legacy sites. This approach promotes cleaner production practices and supports climate resilience in the context of contaminated land management.

CRediT authorship contribution statement

Subin Babu: Writing – original draft, Validation. **Fengqing Li:** Writing - methods and results, Visualization, Software, Investigation, Validation, Methodology, Conceptualization. **Petra Schneider:** Writing - methods and results, review & editing, Supervision, Funding acquisition, Data curation, Validation, Resources, Methodology, Formal analysis, Conceptualization.

Declaration of Competing Interest

The authors declare the following financial interests/personal relationships which may be considered as potential competing interests:

Petra Schneider reports financial support, administrative support, and article publishing charges were provided by Magdeburg-Stendal University of Applied Sciences. If there are other authors, they declare that they have no known competing financial interests or personal relationships that could have appeared to influence the work reported in this paper.

Acknowledgements

The project "Long-term stability of remediated waste heap piles from uranium mining" was financed by the Saxon State Office for the Environment, Agriculture and Geology (project duration: 03/2020–09/2022).

Data Availability

Data will be made available on reasonable request.

References

[1] Lange, G., Muehlstedt, P., Freyhoff, G., Schroeder, B., 1991. Uranium mining in Thuringia and Saxony - a survey of geology and mining. Erzmetall 44 (3), 162–171.
[2] Al-Akel, S.; Kunze, C..Müller, M., Schneider, P.: Long-term stability of rehabilitated uranium mining heaps - Report on work package 1. {C}L.F.U.L.G.{C} (ED.), Dresden, September 2020.
[3] Hajo Zeeb, Ferid Shannoun World Health Organization (WHO) Handbook on Indoor Radon - a public health perspective, edited by 2009, 13-14.
[4] Przydatek, G., Generowicz, A., Kanownik, W., 2024. Evaluation of the activity of a municipal waste landfill site in the operational and non-operational sectors based on landfill gas productivity. Energies 17, 2421. https://doi.org/10.3390/en17102421.
[5] Hartley, J.N., Koehmstedt, P.L., Esterl, D.J., 1980. Asphalt emulsion sealing of uranium mill tailings (S). Plenum Press, pp. 681–688 (S).
[6] Ozbay, Gulnihal, Jones, Morgan, Gadde, Mohana, Isah, Shehu, Attarwala, Tahera, 2021. Design and operation of effective landfills with minimal effects on the environment and human health, 2021 J Environ Public Health 6921607, 13. https://doi.org/10.1155/2021/6921607.
[7] Scheutz, C., Mosbæk, H., Kjeldsen, P., 2004. Attenuation of methane and volatile organic compounds in landfill soil covers. J Environ Qual 33, 61–71. https://doi.org/10.2134/jeq2004.6100.
[8] Chenhua Wang, Junjie Liu, Chuck Wah Yu, Dong Xie, 2022. Numerical analysis for the optimization of multi-parameters stratum ventilation and the effect on radon dispersion. ISSN 2352-7102 J Build Eng 62, 105375. https://doi.org/10.1016/j.jobe.2022.105375.
[9] Manheim, D.C., Yeşiller, N., Hanson, J.L., 2021. Gas emissions from municipal solid waste landfills: a comprehensive review and analysis of global data. J Indian Inst Sci 101, 625–657. https://doi.org/10.1007/s41745-021-00234-4.
[10] Albright, W.H., Benson, C.H., Gee, G.W., Abichou, T., Tyler, S.W., Rock, S.A., 2006. Field performance of three compacted clay landfill covers. Vadose Zone J 5, 1157–1171. https://doi.org/10.2136/vzj2005.0134.
[11] Manheim, Derek C., Yesiller, Nazli, Hanson, James L., 2021. Climate Change Effects of Gases from Municipal Solid Waste Landfills, 9. Japanese Geotechnical Society Special Publication, pp. 142–147. https://doi.org/10.3208/jgssp.v09.cpeg035.
[12] Roesel, Lydia K., 2022. Effects of less impermeable sealings for mine piles. ISSN 0925-8574 Ecol Eng 176, 106515. https://doi.org/10.1016/j.ecoleng.2021.106515.
[13] Hotton, G., Bussière, B., Pabst, T., et al., 2020. Influence of climate change on the ability of a cover with capillary barrier effects to control acid generation. Hydrogeol J 28, 763–779. https://doi.org/10.1007/s10040-019-02084-y.
[14] Beck-Broichsitter, S., Fleige, H., Gerke, H.H., Horn, R., 2020. Effect of artificial soil compaction in landfill capping systems on anisotropy of air-permeability. J Plant Nutr Soil Sci 183, 144–154. https://doi.org/10.1002/jpln.201900281.
[15] Hanson, James L., Manheim, Derek C., Yeşiller, Nazli, 2023. Geoenvironmental assessment of climate impacts from landfill gas emissions. ISSN 0038-0806 Soils Found 63 (2), 101279. https://doi.org/10.1016/j.sandf.2023.101279.
[16] Xuan Ling, Wei Chen, Katrin Schollbach, H.J.H. Brouwers, Low permeability sealing materials based on sewage, digestate and incineration industrial by-products in the final landfill cover system, Construction and Building Materials, Volume 412, ISSN 0950-0618, https://doi.org/10.1016/j.conbuildmat.2024.134889.
[17] Kawther, Al-Soudany, Mohammed, Fattah, Falah, Rahil, 2024. A Rev Land Liner Liner Syst. https://doi.org/10.1063/5.0212198.
[18] Daramola, S.O., Hingston, E.D.C., Demlie, M., 2024. A review of lateritic soils and their use as landfill liners. Environ Earth Sci 83, 118. https://doi.org/10.1007/s12665-023-11392-2.
[19] Stojanovic, M., Milojkovic, Jelena, 2011. Phytoremediation of uranium contaminated soils. Handb Phytoremediat 93–136.
[20] Sheoran, A.S., Sheoran, V., 2006. Heavy metal removal mechanism of acid mine drainage in wetlands: a critical review. ISSN 0892-6875 Miner Eng 19 (2), 105–116. https://doi.org/10.1016/j.mineng.2005.08.006.
[21] Schneider, P., Osenbrück, K., Neitzel, P.L., Nindel, K., 2002. In-situ mitigation of effluents from acid waste rock dumps using reactive surface barriers - a feasibility study. J Mine Water Environ Top Issue Large Scale Model Environ 21 (2002), 36–44.
[22] Schneider, P., Neitzel, P.L., Osenbrück, K., Noubacteb, C., Merkel, B., Hurst, S., 2001. In-situ treatment of radioactive mine water using reactive materials - results of lab and field experiments in uranium ore mines in Germany. In: In: Hydrochimica et hydrobiologica Acta, 29, pp. 1–10. https://doi.org/10.1002/1521-401X(200109)29:2/3<129::AID-AHEH129>3.0.CO;2-2, 2.
[23] Barnekow, U. et.al. (2013): Fifteen years of design, construction and monitoring of soil covers on Wismut´s uranium mining legacy sites, a synopsis, ⟨https://papers.acg.uwa.edu.au/p/1352_10_Barnekow/⟩, 12.06.2020.
[24] Klaus Berger, Alexander Groengroeft, Julia Gebert, 20 years performance measurements of a landfill cover system with components constructed from pre-treated dredged sediments, Waste Management, Volume 100, Pages 230-239, https://doi.org/10.1016/j.wasman.2019.09.016.
[25] Bister, S., Birkhan, J., Lüllau, T., Bunka, M., Solle, A., Stieghorst, C., Riebe, B., Michel, R., Walther, C., 2015. Impact of former uranium mining activities on the floodplains of the Mulde River, Saxony, Germany. ISSN 0265-931X J Environ Radioact 144, 21–31. https://doi.org/10.1016/j.jenvrad.2015.02.024.
[26] Paul R., Schroeder, Thomas S. Dozier, Paul A. Zappi, Bruce M. McEnroe, John W. Sjostrom and R. Lee Peyton, The Hydrologic Evaluation of Landfill Performance (HELP) Model, Engineering Documentation for Version 3; U.S. Risk Reduction Engineering laboratory office of research and development. US Environmental Protection Agency, Interagency equipment number – DW21931425, 115-120.
[27] Chabuk, Ali, Al-Ansari, Nadhir, Mohammad, Mohammad, Jan, Laue, Roland, Pusch, Hussain, Hussain, Sven, Knutsson, 2018. Two scenarios for landfills design in special conditions using the HELP model: a case study in Babylon Governorate, Iraq. Sustainability. https://doi.org/10.3390/su10010125.
[28] Alslaibi, T.M., Abustan, I., Mogheir, Y.K., Afifi, S., 2013. Quantification of leachate discharged to groundwater using the water balance method and the hydrologic evaluation of landfill performance (HELP) model. Waste Manag Res 31 (1), 50–59. https://doi.org/10.1177/0734242X12465462.
[29] Liu, X., Li, X., Lan, M., et al., 2021. Experimental study on permeability characteristics and radon exhalation law of overburden soil in uranium tailings pond. Environ Sci Pollut Res 28, 15248–15258. https://doi.org/10.1007/s11356-020-11758-0.
[30] Espósito, Rogério O., Castier, Marcelo, Tavares, Frederico W., 2000. Calculations of thermodynamic equilibrium in systems subject to gravitational fields. ISSN 0009-2509 Chem Eng Sci 55 (17), 3495–3504. https://doi.org/10.1016/S0009-2509(00)00010-5.
[31] Sanchez-Vila, X., Guadagnini, A., Carrera, J., 2006. Representative hydraulic conductivities in saturated groundwater flow. RG3002 Rev Geophys 44. https://doi.org/10.1029/2005RG000169.
[32] Saâdi, Zakaria, Jérôme, Guillevic, 2016. Comparison of two numerical modelling approaches to a field experiment of unsaturated radon transport in a covered uranium mill tailings soil (Lavaugrasse, France). ISSN 0265-931X J Environ Radioact 151 (Part 2), 361–372. https://doi.org/10.1016/j.jenvrad.2015.03.019.
[33] Heinze, M., Sänger, H., 1996. Die Durchwurzelung künstlicher Rohböden auf Halden - Erste Erkenntnisse von Untersuchungen im Bereich des thüringisch-sächsischen Uranbergbaus (Root penetration of artificial raw soils on heaps - first findings from investigations in the Thuringian-Saxon uranium mining sector). In: Geowissenschaften (Berlin), 14, pp. 467–469.
[34] Berger, K., 1998. Validierung und Anpassung des Simulationsmodells HELP zur Berechnung des Wasserhaushalts von Deponien für deutsche Verhältnisse (Validation and adaptation of the simulation model HELP for calculating the water balance of landfills for German conditions. Environmental Protection Agency, Germany.
[35] Berger, K., Schroeder, P.R., 2013. Das Hydrologic Evaluation of Landfill Performance (HELP) Modell. Benutzerhandbuch für HELP-D (Version 3.95 D). 6., vollständig überarbeitete Auflage. Institut für Bodenkunde der Universität Hamburg. Geo Universität Hamburg.
[36] Berger, K., 2015. On the current state of the hydrologic evaluation of landfill performance (HELP) model. Waste Manag 38, 201–209.
[37] ad-hoc-Arbeitsgruppe Boden, 2005. Bodenkundliche Kartieranleitung. KA5 / Soil science mapping guide. In: KA5 (Ed.), Bundesanstalt für Geowissenschaften und Rohstoffe in Zusammenarbeit mit den Staatlichen Geologischen Diensten, 5. verbesserte u. erweiterte Auflage.
[38] C&E Consulting und Engineering GmbH (1998). Project support for the Aue waste dump remediation facility. Final report: Preparation of a suitability assessment for the three proposed subsoil material variants and monitoring of the field trials for the waste dump remediation technology at the Schlema-Alberoda site, from the trial implementation to the final report (in German)., 11.12.1998, non public.
[39] C&E Consulting und Engineering GmbH (1998). Report on the topic: Water balance assessment of test fields Borbachdamm (in German), 30.11.1998, non public.
[40] C&E Consulting und Engineering GmbH (2012). Final report on the performance of data evaluation and model comparison for soil measurement stations in the Aue branch 2011 (in German), 13.05.2012, non public.
[41] Deutsche Vereinigung für Wasserwirtschaft und Kulturbau e.V. DVWK, 1996. Deponieabdichtungen in Asphaltbauweise (Landfill sealing in asphalt construction). Nr. 237/1996. In: Merkblatt, 1996. Verlag Paul Parey, Hamburg.

[42] Forschungsinstitut für Bergbaufolgelandschaften e.V (1998). Final report: Monitoring of field trials on the Borbachdamm spoil heap at the Schlema-Alberoda site on topsoil production technology, 15.12.1998, non public.
[43] Bauberatung Geokunststoffe (2009). Input values for HELP analysis for selected Secudrain drainage mats (in German, NAUE GmbH & Co KG), non public.
[44] Baldauf (2005): Baldauf, S.; Tarnowski, C.: Assessment of the long-term behaviour of PEHD geomembranes based on project-related experience and evidence (in German). In: {C}SKZ-ConSem GmbH & A.K. GWS{C}: 21. Fachtagung „Die sichere Deponie“, Würzburg, 10./11.02.2005.
[45] Landesamt für Natur, Umwelt und Verbraucherschutz Nordrhein-Westfalen LANUV, 2015. Technische Anforderungen und Empfehlungen für Deponieabdichtungssysteme, Konkretisierungen und Empfehlungen zur Deponieverordnung, LANUV-Arbeitsblatt 13 13 available online: ⟨https://www.lanuv.nrw.de/fileadmin/lanuvpubl/4_arbeitsblaetter/40013.pdf⟩.
[46] Müller, W. (2009). Dichtungsbahnen zur Abdichtung von Deponien und Altlasten. In: SKZ-ConSem GmbH & AK GWS (Veranstalter): 25. Fachtagung „Die sichere Deponie“, Würzburg, 26./27.02.2009.
[47] Olischläger, V.; Maubeuge, K. (2006): Chancen für BAM-zugelassene Dichtungsbahnen bei Projekten im europäischen Ausland. In: SKZ-ConSem GmbH & AK GWS (Veranstalter): 22. Fachtagung „Die sichere Deponie“, Würzburg, 16./17.02.2006.
[48] Tolaymat, T.; Krause, M. (2020). Hydrologic Evaluation of Landfill Performance HELP 4.0 User Manual, available online: ⟨https://www.epa.gov/land-research/help-40-user-manual⟩.
[49] Zentrum für angewandte Forschung und Technologie ZAFT e. V. an der HTW Dresden, Fachgebiet Geotechnik (2020). Bericht Nr. 20113zl, Labor-Bericht: Prüfergebnisse Ersatzbaustoffe, 15.12.2020, non public.
[50] Huesker Synthetic GmbH (2013). Vliesstoff HaTe Typ B 400 „O“ II, Produktbeschreibung.
[51] NAUE GmbH & Co.K.G. (2011). Multifunktionale Filter- und Trennvliesstoffe – SecutexR PPweiß, Produktbeschreibung.
[52] Bayerisches Landesamt für Umwelt, 2014. Bewertung von Entwässerungsschichten in Oberflächenabdichtungen von Deponien und Altablagerungen, Merkblatt Nr. 3.6/5. Stand Oktober 2014 available online: ⟨https://www.lfu.bayern.de/wasser/merkblattsammlung/teil3_grundwasser_und_boden/doc/nr_365.pdf⟩.
[53] Arbeitskreis 2.3 der GDDT, 2015. GüteRLAsphalt Güterichtlinie für Abdichtungskomponenten aus Deponieasphalt. Deutsche Gesellschaft für Geotechnik e.V. Arb 2 3 Asph Im Wasserbau und der Geotech 1, 2015 (Ausgabe).
[54] Hundhausen, U. (2005). Asphaltabdichtungen als Oberflächenabdichtungen – eine Alternative zur Kunststoffdichtungsbahn?. SKZ-ConSem GmbH & AK GWS: „Die sichere Deponie“, Würzburg, 10./11.02.2005, available online: ⟨https://www.akgws.de/sites/default/files/h_hundhausen.pdf⟩.
[55] Kudla, W.; Dahlhaus, F.; Glaubach, U.; Gruner, M.; Haucke, J. (2009). Diversitäre und redundante Dichtelemente für langzeitstabile Verschlussbauwerke, Abschlussbericht TU Bergakademie Freiberg zum Vorhaben 02C1124, finanziert durch das Bundesministerium für Bildung und Forschung, available online: ⟨https://tu-freiberg.de/sites/default/files/media/professur-fuer-erdbau-und-spezialtiefbau-4411/Publikationen/02c1124.pdf⟩.
[56] LAGAAsphalt (2020): LAGA ad-hoc-AG Deponietechnik: Eignungsbeurteilung von Deponieasphalt zur Basis- und Oberflächenabdichtung von Deponien vom 02.03.2015. Fortschreibung am 03.12.2019, veröffentlicht am 02.03.2020, available online: ⟨https://www.laga-online.de/Publikationen-50-Informationen-Bundeseinheitliche-Eignungsbeurteilungen.html⟩.